Supporting information

Unveiling a Pyridine-Based Exciplex Host for Efficient Stable Blue Phosphorescent Organic Light-Emitting Diodes

Subramanian Muruganantham[1], Young Hun Jung[1], Hye Rin Kim[1], Jung Ho Ham[1], Ramanaskanda Braveenth[1], Kenkera Rayappa Naveen[1], Mi Young Chae[1] and Jang Hyuk Kwon[1]**

[1]Organic Optoelectronic Device Lab. (OODL), Department of Information Display
Kyung Hee University 26, Kyungheedae-ro, Dongdaemun-gu, Seoul 02447, Republic of Korea

**Corresponding Authors*: Mi Young Chae (mychae@khu.ac.kr) and Jang Hyuk Kwon (jhkwon@khu.ac.kr)

Contents

4. Table

5. References

1. Experimental Section

1.1 General Synthetic Materials & Methods: All reagents were purchased from commercial sources, Sigma Aldrich, TCI Chemicals and SK chemicals. The Solvents are analytical grade and were used without further purification unless otherwise stated. All the chemical reactions were carried out under oven-dried flasks in an inert atmosphere. All reaction progress was screened and confirmed by using thin-layer chromatography ((pre-coated TLC Silica gel 60G F_{254} 25 Glass plates 20 x 20 cm and under UV illumination at 254 nm for UV active materials was visualized. The Silica filtration and purification process used silica gel 60-120 with a mesh. 1,4,5,8,9,11-exaazatriphenylene-hexacarbonitrile (HATCN), N-(1,1′-biphenyl-4-yl)-N-[4-(9-phenyl-9H-carbazol-3-yl)phenyl]-9,9-dimethyl-9H-fluoren-2-amine (PCBBiF), 1,3-bis(9-phenyl-1,10-phenanthrolin-2-yl)benzene (BBPB) was purchased from sigma Aldrich, luminescence technology and 2,2'-di(9H-carbazol-9-yl)-1,1'-biphenyl (*o*CBP) and 2,4-bis(dibenzo[*b,d*]furan-2-yl)-6-phenyl-1,3,5-triazine (DDBFT) were synthesised following the previously reported procedures. [1,2]

1.2. Theoretical calculations: Density functional theory (DFT) calculation for the optimization of the ground state and the time dependent-DFT (TD-DFT) for the excited state geometry were predicted with the function and basis set of the Lee–Yang–Parr correlation functional (B3LYP)/6-31(G)** by using the Schrodinger 2023-1 program. A similar approach and function were used to calculate the HOMO-LUMO distribution, energy levels, singlet and triplet and dipole moment etc. Molecular dynamics simulations were also carried out using a Schrödinger Material Science 5.0 program and performed using a Desmond MD engine. A disordered system consists of molecules. For molecules, 10 conformers were selected in the most stable order, and the number was selected according to the Boltzmann population ratio. This disordered system was stabilized by using the material relaxation protocol. It consisted of a 20 ps NVT Brownian minimization at 10 K, a 20 ps NPT Brownian minimization at 100 K, and then a 100 ps NPT MD stage at 300 K. After that, the MD simulation time was kept 100 ns at 300 K and 1 atm. 100 dimers were extracted randomly in the MD simulation. The electron coupling factor of dimers was calculated using B3LYP/LACV3P**.

The optical simulation of OLEDs was carried out using the SETFOS 5.1 (Fluxim) program. The refractive index, extinction coefficient, photoluminescence spectrum of EML, and thickness of each layer were used as input parameters.

1.3. Measurements: Photophysical properties characterization of all materials were prepared in an analytical grade toluene solution at a concentration of $1x10^{-4}$ - 1×10^{-5} M. The UV-vis absorption (solid-state analysis we used 0.7 mm fused silica substrates) and PL spectra were carried out by a V-750 and FP-8500 spectrophotometer (JASCO). The low temperature (77 K) phosphorescence spectrum was measured by an FP-8500 spectrofluorometer (JASCO). The absolute PLQY values in doped films were measured by connecting an integrating sphere to the same FP-8500 spectrofluorometer. These doped films were also used for measuring transient PL measurements. Cyclic voltammetry (CV) was used to measure the redox potential, three-electrode cell systems such as platinum counter, material coated 150 nm of ITO glass working electrode, and Ag wire in 0.01 M $AgNO_3$ reference electrodes, 0.1 M tetra butyl

ammonium perchlorate (Bu_4NClO_4) as supporting electrolytes in acetonitrile solution respectively. Ferrocene/ferrocenium (Fc/Fc+) was used as the internal standard, the potential values were converted to the saturated calomel electrode scale (EC epsilon electrochemical analysis equipment). Transient PL was carried out when photon counts were reached until 10,000 in a nitrogen atmosphere using a Quantaurus-Tau fluorescence lifetime measurement system (C11367-03, Hamamatsu Photonics. Co). The thermal properties were examined by differential scanning calorimetry (DSC) TA instruments Trios V5.3.0.48151 and thermogravimetric analysis (TGA) TGA Q50 V20.13. The glass transition temperatures (Tg) were determined by the DSC graph, and the decomposition temperatures (Td) were investigated by TGA at 5% weight loss.

1.4. Device fabrication and measurements: The electron only analysis (EOD) device was fabricated without dopant and the device configuration is ITO (50nm)/ BPPB (40 nm)/ Host (30 nm)/ BPPB (40nm)/ Liq (1.5nm)/ Al (100nm), respectively. The phosphorescent OLED device was fabricated in the following configuration: ITO (50nm) /HATCN (7nm)/PCBBiF (45nm)/ *o*CBP (10nm)/ *o*CBP:CNCzPyDFCN or *o*CBP:CNDFPyCzCN 12.wt.% CN-Ir(35nm)/DDBFT(10nm) /BPPB:Liq (30nm)/Liq(1.5nm)/Al. Before the device fabrication, the glass substrates indium-tin-oxide (ITO-coated 50 nm) were cleaned using isopropyl alcohol and acetone in the ultrasonic bath for 10 min and then rinsed with deionized water. The glass substrates were dried using nitrogen and treated in UV-ozone for 10 min. All organic layers and the metal cathode were deposited on the cleaned ITO glass by a vacuum deposition process under a vacuum pressure of 1×10^{-7} Torr. All measurements were carried out under ambient conditions. By the vacuum thermal deposition process organic layers (0.5 Å/s), and the 8-hydroxyquinolinolato-lithium (Liq) were used as the electron injection layer and aluminium (Al) was used as the cathode layer was deposited at the rate of around 0.1, 4.0 Å/s respectively. Finally, completion of the deposition process, the devices were encapsulated with a glass cover and a UV-curable resin under a nitrogen atmosphere to the prevention of moisture issues. J-V, L–V and EQE-L curves were investigated using a Keithley 2635A SMU and Konica Minolta CS-2000 A with luminance and color meters. EL spectra and CIE 1931 color coordinates were obtained from the Konica Minolta CS-2000 spectroradiometer.

1.5. Characterization: To predict the molecular structures of the synthesized materials confirmed by using ^{1}H and ^{13}C NMR, Bruker Avance-400 and 500 Nuclear Magnetic Resonance Spectrometer (NMR). The multiplicity of NMR signals was indicated by s (singlet), d (doublet), t (triplet), dd (doublets of doublet) and m (multiplet) etc., with chemical shift in (ppm) and $CDCl_3$ was used as a solvent, TMS tetra methyl silane was used as internal standard. High-resolution mass spectra were performed using a JEOL MS-700 Gas Chromatography Mass spectrometer. High-performance liquid chromatography (HPLC) was used to measure the material purities and further sublimated by high atmospheric temperature to improve the purity of the compound and aid in vacuum deposition during the device operation.

1.6. Synthesis

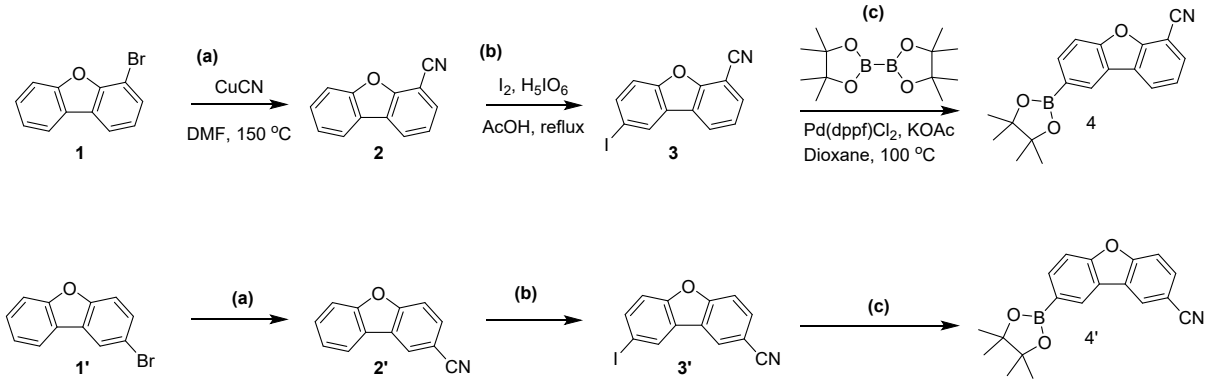

Scheme S1. Synthesis of intermediates **4** and **4′**.

The intermediates **2,2'** to **4, 4'** were synthesized according to the previously reported synthetic procedures.[3-4]

Synthesis of dibenzo[b,d]furan-4-carbonitrile (2): 4-bromodibenzo[*b,d*]furan (3.00 g, 12.14 mmol) and copper cyanide (CuCN) (2.17 g, 24.28 mmol) were stirred in dimethylformamide (DMF, 250 mL) stirred under nitrogen atmosphere and further refluxed 12 h. After completion of the reaction mixture (confirmed TLC) cooling to room temperature and filter through silica/ celite bed and the filtrate was extracted, dichloromethane, aqueous ammonia solution of 50 mL was added. Then the organic layer was washed with aqueous NaCl solution three times and dried over $MgSO_4$. Then the solvent was removed under vacuum and the crude product was purified by column chromatography using a silica gel column with MC/Hexane as eluents (1:3). The purified compound **(2)** was obtained as a white solid. Yield: 1.6g, 68.4%, ^{1}H NMR (500 MHz, $CDCl_3$, room temperature) δ (ppm): 8.09 (dd, J_1 = 7.9; J_2 = 0.9 Hz, 1H), 7.90 (d, J = 7.7 Hz, 1H), 7.65 (dd, J_1 = 7.4; J_2 = 0.8 Hz, 1H), 7.60 (d, J = 8.2 Hz, 1H), 7.52-7.50 (m, 1H), 7.40-7.35 (m, 2H).

Synthesis of 8-iododibenzo[b,d]furan-4-carbonitrile (3): To the mixture of compound **(2)** (3.00 g, 15.53 mmol), periodic acid (H_5IO_6) (3.89 g, 17.08 mmol), and I_2 (4.34 g, 17.08 mmol) were added into acetic acid (120 mL) stirred under nitrogen atmosphere at refluxed condition. After completion of the reaction cooling to room temperature, the mixture was poured into cold water (300 mL), separated into 400 mL of dichloromethane, washed with aqueous sodium thiosulphate, and evaporated the solvent. The crude product was purified by column chromatography with a mixture eluent of MC/Hexane (1:5), compound **(3)** obtained as a white solid. Yield: 1.4 g, 65.0%. ^{1}H NMR (500 MHz, $CDCl_3$, room temperature) δ (ppm): 8.25 (d, J = 1.7 Hz, 1H), 8.08 (dd, J_1 = 7.9; J_2 = 1.05 Hz, 1H), 7.80 (dd, J_1 = 8.6; J_2 = 1.7 Hz, 1H), 7.73 (dd, J_1 = 7.9; J_2 = 0.9 Hz, 1H), 7.44-7.41 (m, 2H).

Synthesis of 8-(4,4,5,5-tetramethyl-1,3,2-dioxaborolan-2-yl)dibenzo[b,d]furan-4-carbonitrile (4): A mixture of 8-iododibenzo[*b,d*]furan-4-carbonitrile (**3**) (5.0 g, 15.62 mmol), 4,4,4',4',5,5,5',5'-octamethyl-2,2'-bi(1,3,2-dioxaborolane) (5.95 g, 23.44 mmol), potassium acetate (4.61 g, 47.0 mmol), $Pd(dppf)Cl_2$ (0.68 g, 0.93 mmol), and 60 mL of 1,4-dioxane were stirred at 100 °C for 12 h under nitrogen atmosphere. After the reaction mixture was cooled to room temperature and filtered through a silica and celite bed, the solution was extracted by

water/dichloromethane three times, and then the organic layer dried over $MgSO_4$ and the solvent was evaporated under reduced pressure. The crude product was purified by column chromatography on a silica gel column, and the eluent MC/Hexane (1:4) obtained intermediate **(4)** as a white solid. Yield: 3.7g, 74.0%. ^{1}H NMR (500 MHz, $CDCl_3$) δ (ppm): 8.43 (s, 1H), 8.14 (d, J = 7.4 Hz, 1H), 7.98 (d, J = 8.1 Hz, 1H), 7.68 (d, J = 7.6 Hz, 1H), 7.63 (d, J = 8.3 Hz, 1H), 7.40 (t, J = 7.0 Hz, 1H), 1.38 (s, 12H).

Synthesis of dibenzo[b,d]furan-2-carbonitrile (2')*:** 2-bromodibenzo[*b,d*]furan (5.0 g, 20.23 mmol) and CuCN (3.62 g, 40.47 mmol) was dissolved in DMF stirred under nitrogen atmosphere and further refluxed 12 h. After completion of the reaction cooling to room temperature, dichloromethane 500 mL and distilled water 300 mL were added and the organic phase was separated. The product was purified via silica gel column chromatography with MC/hexane (1:4) as eluent, and ***2' was obtained as a white powder, Yield: 2.8 g, 72.0%. ^{1}H NMR (400 MHz, $CDCl_3$, room temperature) δ (ppm): 8.23 (d, J = 2.4, 1H), 7.96-7.94 (m, 1H), 7.71 (dd, J_1 = 8.6 Hz, J_2 = 1.8 Hz 1H), 7.62-7.7.59 (m, 2H), 7.55-7.52 (m, 1H), 7.42-7.739 (m, 1H).

Synthesis of 8-iododibenzo[b,d]furan-2-carbonitrile (3')*:** Under nitrogen atmosphere compound ***2' (3.0 g, 15.53 mmol), periodic acid (H_5IO_6) (3.89 g, 17.08 mmol), and I_2 (4.34 g, 17.08 mmol) were added into acetic acid (120 mL) stirred at refluxed condition. After completion of the reaction cooling to room temperature, dichloromethane 250 mL and distilled water 150 mL were added, and the organic phase was separated. The crude product was purified by column chromatography with a mixture eluent of MC/Hexane (1:5), compound ***(3')*** obtained as a white solid, Yield: 1.62 g, 75.0%. ^{1}H NMR (400 MHz, $CDCl_3$, room temperature) δ (ppm): 8.30 (s, 1H), 8.23 (s, 1H), 7.84-7.76 (m, 2H), 7.66 (d, J_1 = 8.8 Hz, J_2 = 1.2 Hz, 1H), 7.40 (d, J = 8.8 Hz, 1H).

Synthesis of 8-(4,4,5,5-tetramethyl-1,3,2-dioxaborolan-2-yl)dibenzo[b,d]furan-2-carbonitrile (4'): Under nitrogen atmosphere compound 8-iododibenzo[*b,d*]furan-2-carbonitrile (**3**) (5.0 g, 15.62 mmol), 4,4,4',4',5,5,5',5'-octamethyl-2,2'-bi(1,3,2-dioxaborolane) (5.95 g, 23.44 mmol), potassium acetate (4.61 g, 47.0 mmol), $Pd(dppf)Cl_2$ (0.68 g, 0.93 mmol), and 60 mL of 1,4-dioxane were stirred at 100 °C for 12 h under nitrogen atmosphere. After cooling to room temperature, dichloromethane 400 mL and distilled water 250 mL were added, and the organic phase was separated. The crude product was purified by column chromatography with a mixture eluent of MC/Hexane (1:3), compound ***(3')*** obtained as a white solid, Yield: 2.1 g, 70.0%. ^{1}H NMR (400 MHz, $CDCl_3$, room temperature), δ (ppm): 8.46 (s, 1H), 8.27 (s, 1H), 8.0 (d, J = 8.4 Hz, 1H), 7.74 (d, J = 8.4 Hz, 1H), 7.66-7.60 (m, 2H), 1.40 (s, 12H).

Synthesis of 9-(4-bromopyridin-2-yl)-9H-carbazole-3-carbonitrile (7): 9*H*-carbazole-3-carbonitrile (3.27 g, 1.0 mmol) and 45 mL of dry DMF were added to an oven-dried 100 mL three-necked round bottom flask under nitrogen atmosphere at 0 °C; thereafter, NaH (0.89 g, 37.50 mmol) was added. The reaction mixture was slowly warmed to room temperature and stirred for 30 minutes. The 2-bromo-6-fluoropyridine (3g, 17.04 mmol) dissolved in 5 mL of dry DMF solution was added dropwise, and then the reaction mixture was stirred at 150 °C for 6 h. The completion of the reaction was cooled to room temperature and quenched with 100 mL of water. The product was extracted with dichloromethane 300 mL, and then the organic layer was washed with water and dried with $MgSO_4$. The solvent was removed under reduced pressure, and then the crude product was purified by column chromatography over a silica gel column. The eluent, MC/Hexane (1:3), was obtained as a white solid intermediate (7). Yield: 3.65 g, 62.0%. ^{1}H NMR (500 MHz, CF_3COOD, room temperature) δ (ppm): 8.60 (d, J = 6.5 Hz, 1H),

8.31 (dd, J_1 = 8.0; J_2 = 0.85 Hz, 2H), 8.07-8.00 (m, 2H), 7.65 (dd, J_1 = 8.6, J_2= 1.5 Hz, 1H), 7.57 (dd, J_1 = 8.5, J_2 = 1.8 Hz, 1H), 7.47-7.37 (m, 3H). ^{13}C NMR (125 MHz, CF_3COOD) δ (ppm): 148.9, 145.1, 141.6, 140.7, 138.8, 130.7, 129.2, 128.8, 127.5, 126.6, 125.9, 125.3, 123.8, 121.4, 110.5, 109.4, 105.6. HRMS (ESI) calcd for $C_{18}H_{10}BrN_3$ $[M]^+$ 347.0058; found, 347.0055.

Synthesis of 9-(2-bromopyridin-4-yl)-9H-carbazole-3-carbonitrile (7'): According to the general procedure from compound **7**, 9*H*-carbazole-3-carbonitrile (3.27 g, 1.0 mmol), NaH (0.89 g, 37.50 mmol) and 2-bromo-6-fluoropyridine (3g, 17.04 mmol) in dry DMF solution then the reaction mixture was stirred at 150 °C for 6 h. The crude product 7' was purified by column chromatography on silica gel eluting with MC/Hexane to afford as a white solid and the yield was 3.4 g, 57.0%. ^{1}H NMR (500 MHz, CF_3COOD) δ (ppm): 8.76 (d, J = 6.8 Hz, 1H), 8.40-8.37 (m, 2H), 8.24 (dd, J_1 = 6.7, J_2 = 2.2 Hz, 1H), 8.07 (d, J = 7.9 Hz, 1H), 7.81-7.74 (m, 2H), 7.67 (d, J = 8.4 Hz, 1H), 7.55-7.52 (m, 1H), 7.47-7.44 (m, 1H). ^{13}C NMR (125 MHz, CF_3COOD, room temperature) δ (ppm): 154.3, 144.6, 138.4, 135.3, 130.5, 128.9, 127.0, 125.6, 125.5, 124.2, 124.2, 121.0, 120.0, 110.0, 105.3. HRMS (ESI) calcd for $C_{18}H_{10}BrN_3$ $[M]^+$, 347.0058; found, 347.0050.

***General procedure for the synthesis of 9-(4-(6-cyanodibenzo[b,d]furan-2-yl)pyridin-2-yl)-9H-carbazole-3-carbonitrile (CNCzPyDFCN)*:** 9-(4-bromopyridin-2-*yl*)-9*H*-carbazole-3-carbonitrile **(7)** (1.0 g, 2.87 mmol) and 8-(4,4,5,5-tetramethyl-1,3,2-dioxaborolan-2-yl)dibenzo[*b,d*]furan-4-carbonitrile **(4)** (1.1 g, 3.44 mmol), 15 mL of 2M K_2CO_3 and tetrakis(triphenylphosphine)palladium (0) ($Pd(PPh_3)_4$ (0.16 g, 0.14 mmol) were stirred in toluene 30 mL and 10 mL ethanol (3:1 ratio) at room temperature for 10 minutes under a nitrogen atmosphere. Then the mixture was refluxed and stirred for 12 h. After completion of the reaction, it was cooled to room temperature, extracted with dichloromethane/water and dried over $MgSO_4$. The solvent was evaporated under vacuo. The crude product CNCzPyDFCN was purified by column chromatography over a silica gel column and the eluent MC/Hexane (1:1) to afford a white solid as a desired product. Yield: 0.72 g, 54.5%). ^{1}H NMR (500 MHz, CF_3COOD, room temperature) δ (ppm): 8.93 (d, J = 6.5 Hz, 1H), 8.61 (d, J = 1.8 Hz, 1H), 8.56 (d, J = 1.6 Hz, 1H), 8.50 (d, J = 1.0 Hz, 1H), 8.40 (dd, J_1 = 6.6; J_2 = 1.7 Hz, 1H), 8.33 (d, J_1 = 7.8; J_2 = 0.8 Hz, 1H), 8.17 (d, J = 7.8 Hz, 1H), 8.13-8.10 (m,1H), 7.9 (d, J = 8.8 Hz, 1H), 7.82-7.80 (m, 2H), 7.75 (d, J = 8.6 Hz, 1H), 7.61-7.60 (m, 2H), 7.55-7.50 (m, 2H). ^{13}C NMR (125 MHz, CF_3COOD) δ (ppm): 159.2, 157.2, 150.6, 150.2, 149.8, 149.5, 145.0, 141.8, 141.1, 139.2, 132.1, 130.6, 129.8, 129.7, 129.0, 128.2, 126.7, 126.2, 126.0, 125.0, 124.8, 124.5, 124.0, 123.6, 122.3, 121.3, 121.0, 110.8, 110.4, 109.3, 105.0, 95.0. MS (ESI) m/z 460 [M]. HR-MS (ESI) calcd for $C_{31}H_{16}N_4O$ [M + H], 460.1324; found, 460.1321. Purity (HPLC): 99.6%.

Synthesis of 9-(2-(8-cyanodibenzo[b,d]furan-2-yl)pyridin-4-yl)-9H-carbazole-3-carbonitrile (CNDFPyDFCN): Compound 9-(2-bromopyridin-4-yl)-9*H*-carbazole-3-carbonitrile **(7')** (1.0 g, 2.87 mmol) and 8-(4,4,5,5-tetramethyl-1,3,2-dioxaborolan-2-yl)dibenzo[b,d]furan-2-carbonitrile **(4')** (1.1 g, 3.44 mmol), 15 mL of 2M K_2CO_3 and $Pd(PPh_3)_4$ (0.16 g, 0.14 mmol) were stirred in toluene 30 mL and ethanol 8 mL (3:1 ratio) and reflux condition for 12 h under nitrogen atmosphere. After completion of the reaction, the crude product CNDFPyDFCN was purified by chromatography on silica gel eluting with MC/Hexane (1:1) to affords the title compound as a white solid (0.80 g, 60.0 %). ^{1}H NMR (500 MHz; CF_3COOD, room temperature) δ (ppm): 9.01 (d, J = 6.7 Hz, 1H), 8.64-8.62 (m, 1H), 8.53 (s, 1H), 8.47 (s, 1H), 8.32-8.31 (m, 1H), 8.20 (d, J = 7.8, Hz, 1H), 8.13 (d, J= 8.6, 1H), 8.0-7.8 (m, 6H), 7.66-7.63 (m, 1H), 7.57 (t, J = 7.6 Hz, 2H). ^{13}C NMR (125 MHz, CF_3COOD)

δ (ppm): 159.7, 155.2, 154.3, 150.2, 149.8, 143.1, 140.8, 132.6, 130.5, 128.9, 127.9, 126.8, 126.1, 125.7, 125.5, 125.0, 124.7, 124.2, 124.0, 121.6, 121, 120.3, 120.0, 114.1, 113.5, 113.1, 110.0, 105.6, 105.0. MS (ESI) m/z 460 [M]. HR-MS (ESI) calcd for $C_{31}H_{16}N_4O$ [M + H], 460.1324; found, 460.1325. Purity (HPLC): 99.49%.

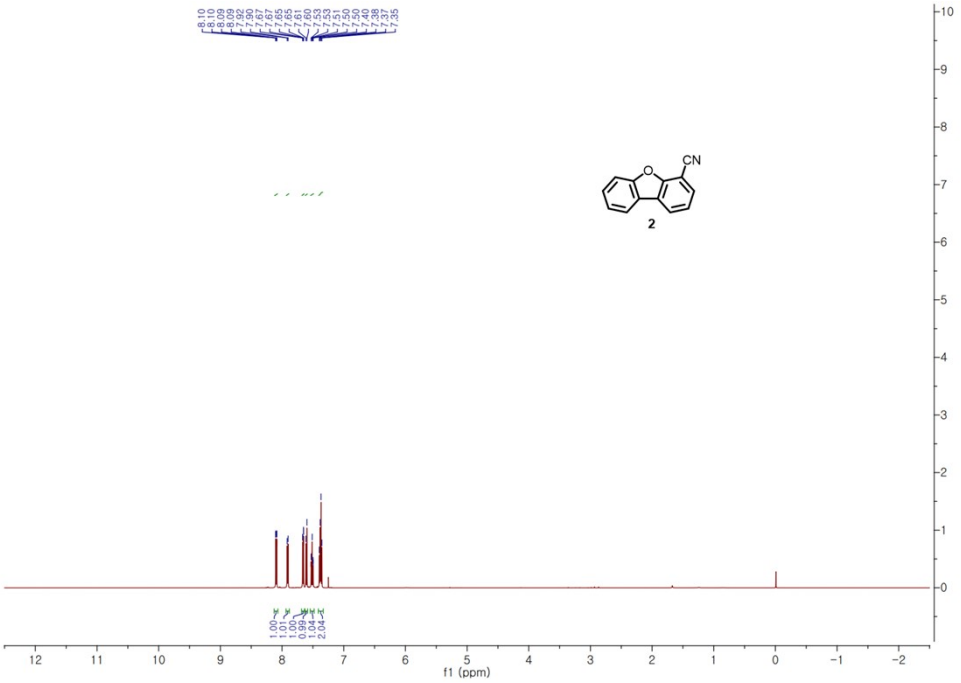

Fig. S1 ^{1}H NMR spectrum for intermediate **2** in $CDCl_3$ (500 MHz).

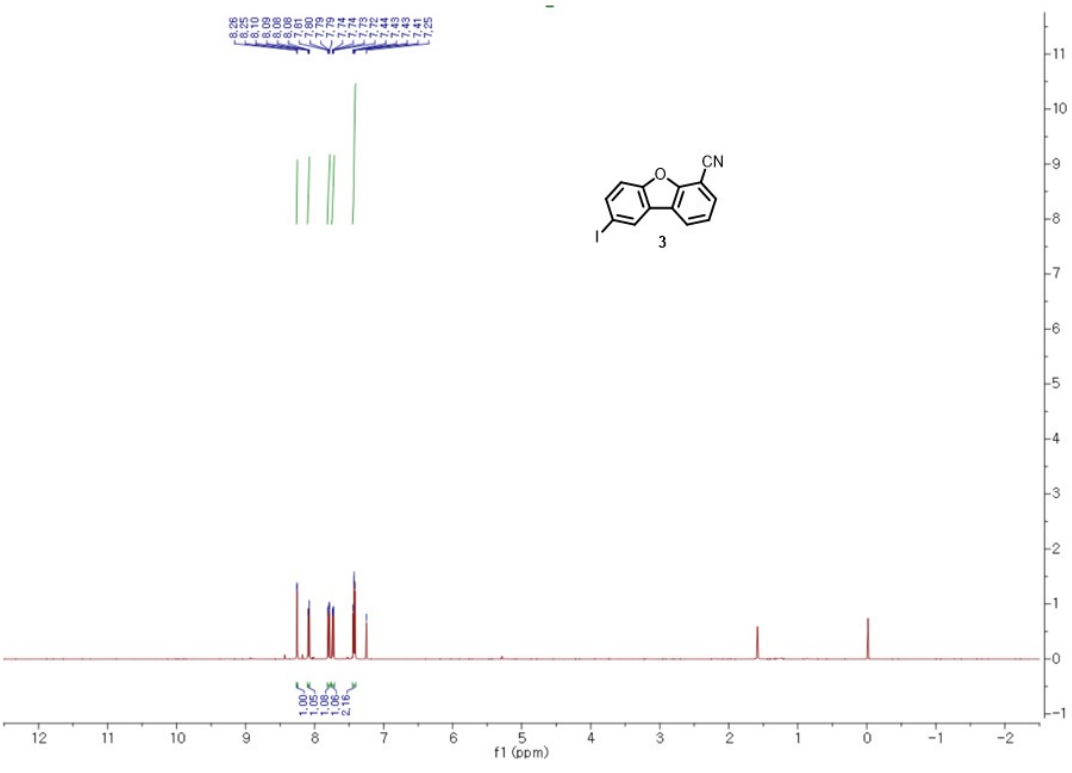

Fig. S2 ^{1}H NMR spectrum for intermediate **3** in $CDCl_3$ (500 MHz).

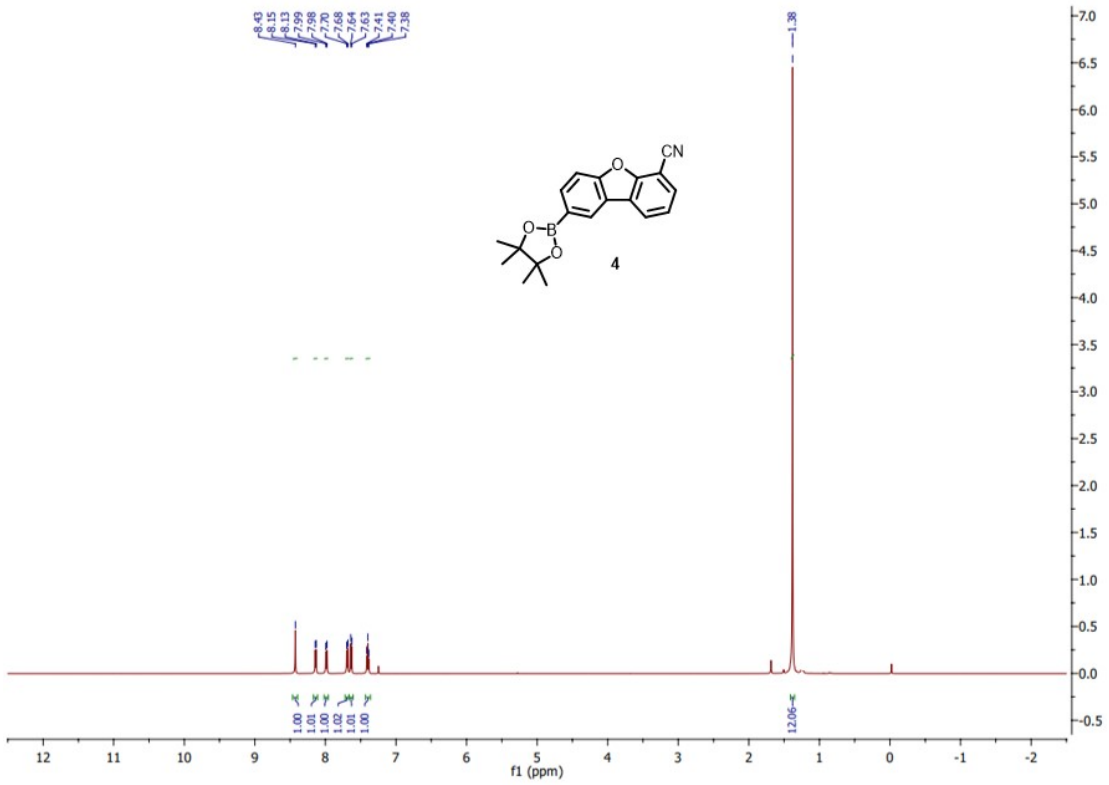

Fig. S3 ^{1}H NMR spectrum for intermediate **4** in $CDCl_3$ (500 MHz).

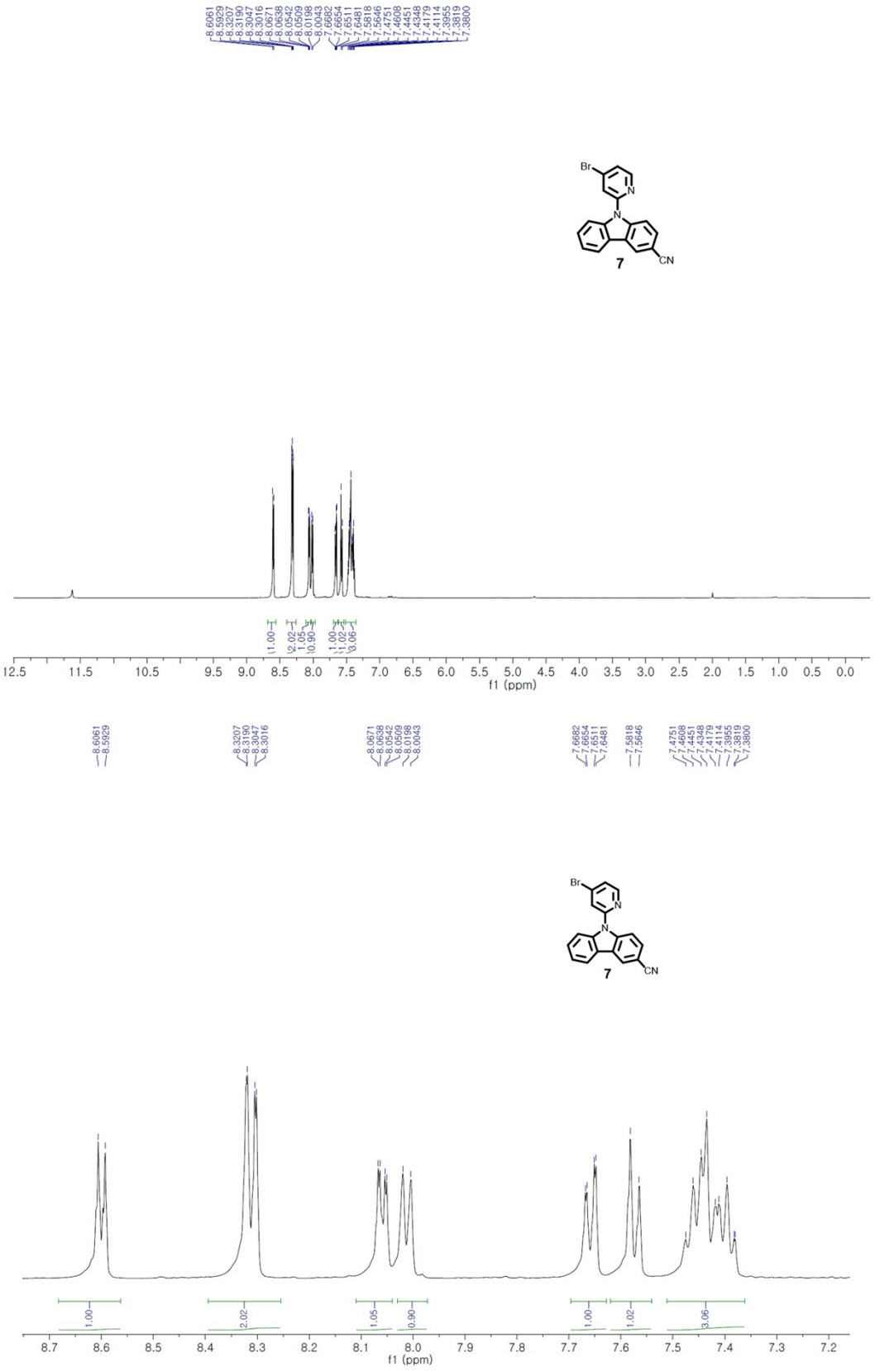

Fig. S4 ^{1}H NMR spectrum for intermediate **7** in CF_3COOD (500MHz).

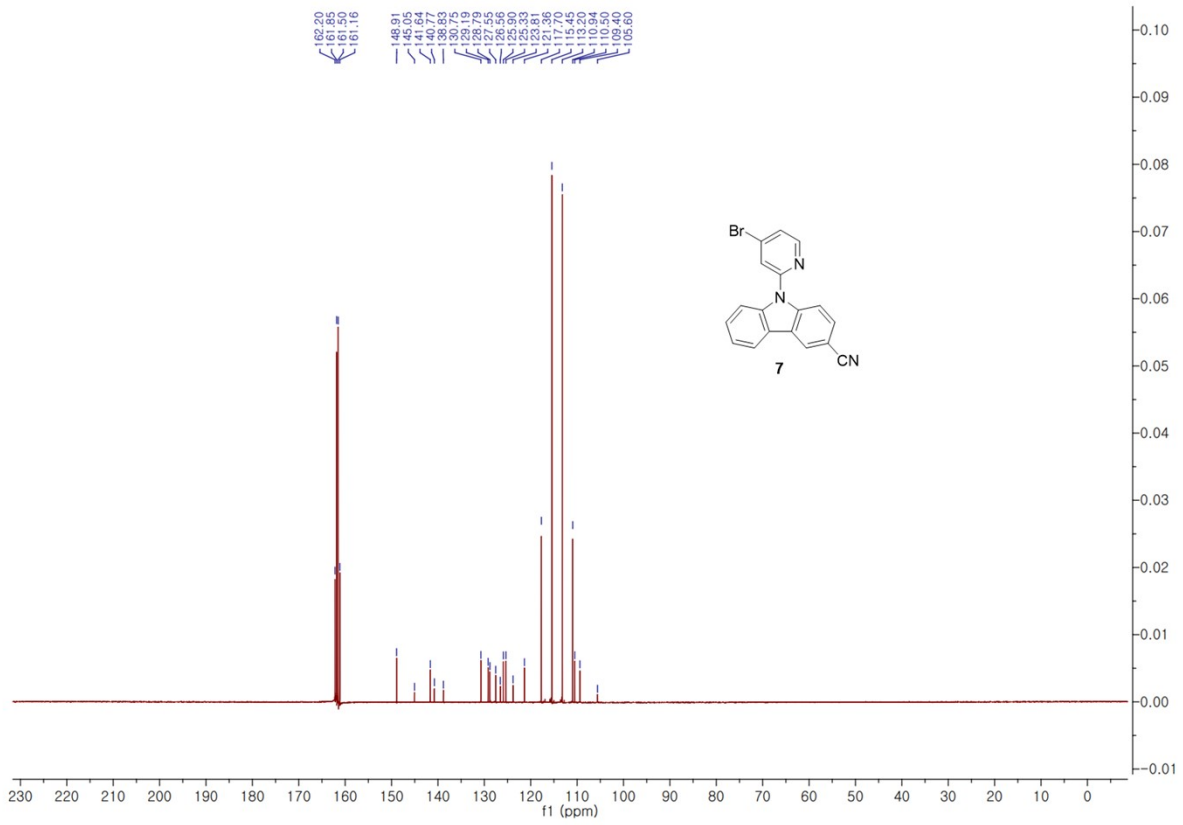

Fig. S5 ^{13}C NMR spectrum of intermediate **7** in CF_3COOD (500 MHz).

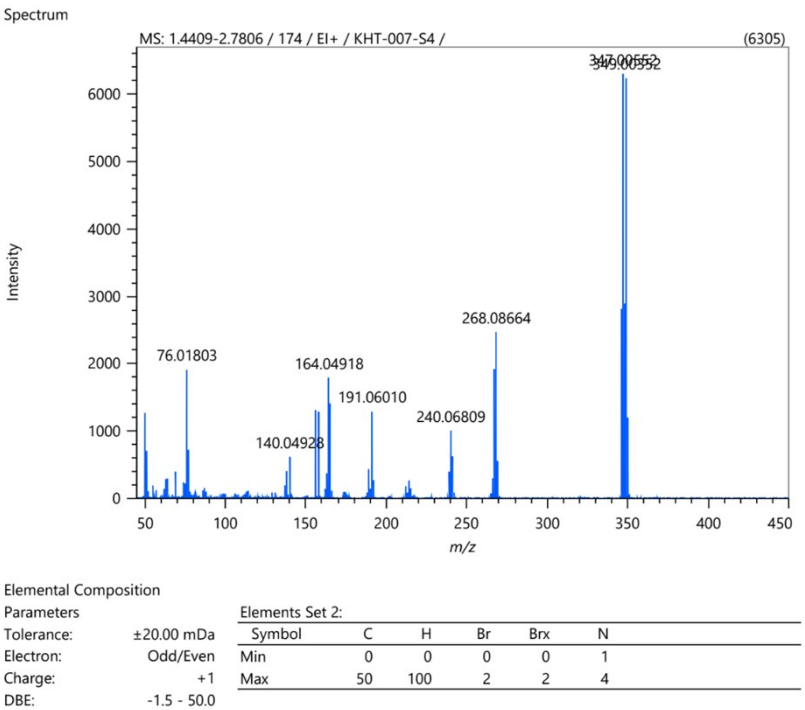

Elemental Composition

Parameters		Elements Set 2:					
Tolerance:	±20.00 mDa	Symbol	C	H	Br	Brx	N
Electron:	Odd/Even	Min	0	0	0	0	1
Charge:	+1	Max	50	100	2	2	4
DBE:	-1.5 - 50.0						

Fig. S6 HRMS spectrum of intermediate **7**.

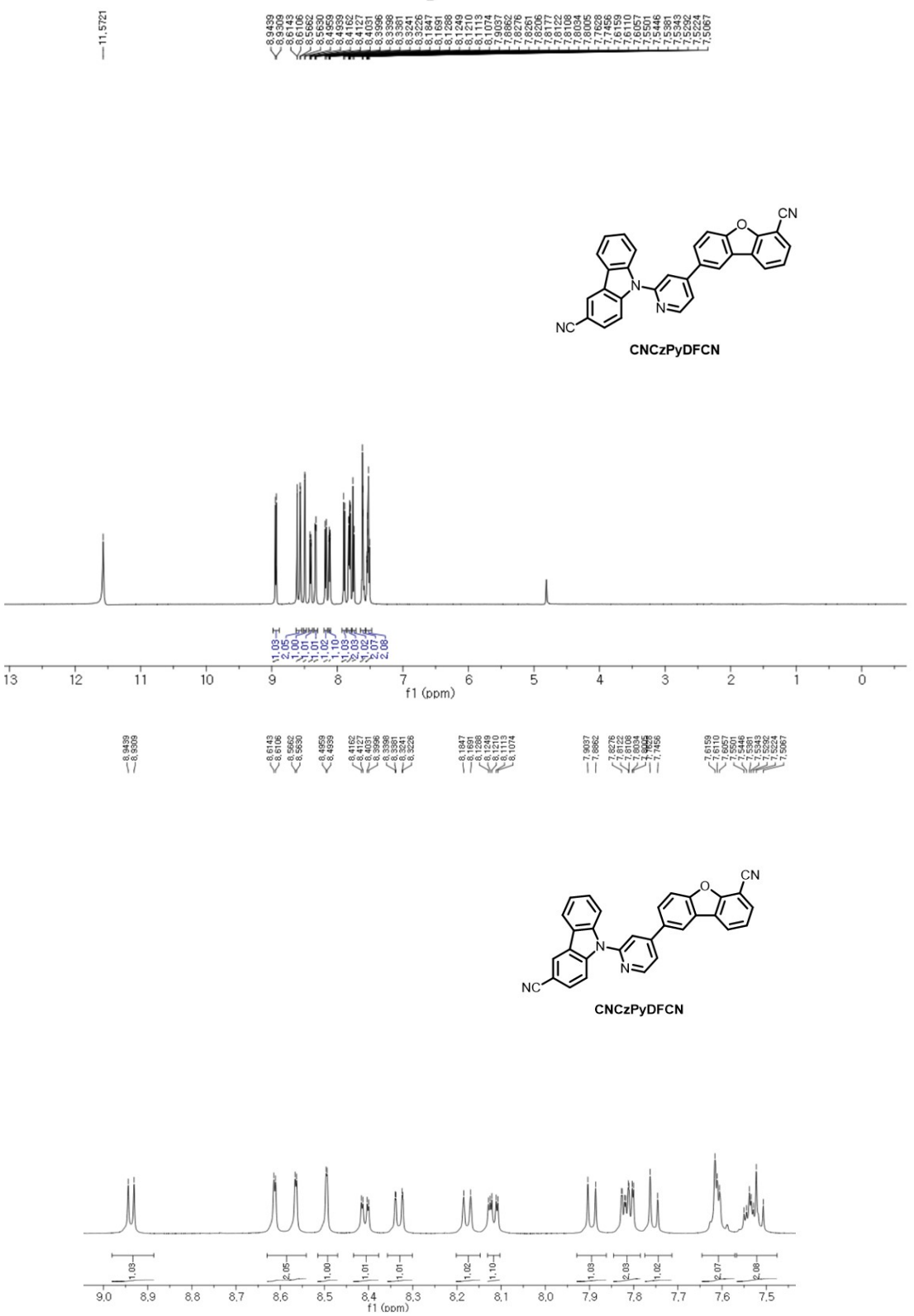

Fig. S7 ^{1}H-NMR spectrum of **CNCzPyDFCN** in CF_3COOD (500 MHz).

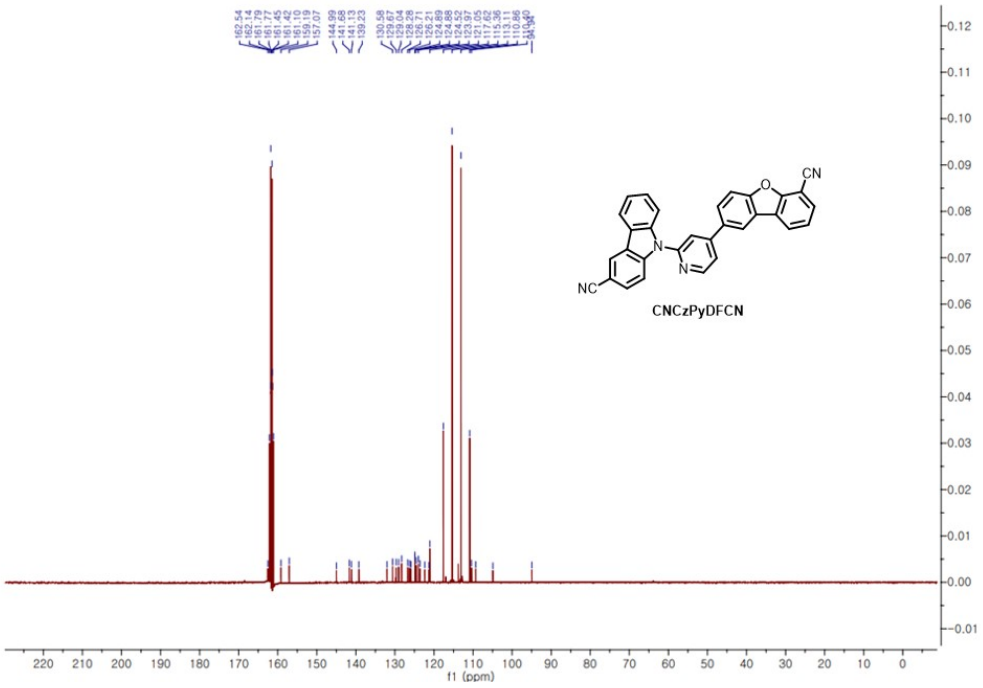

Fig. S8 ^{13}C-NMR spectrum of **CNCzPyDFCN** in CF_3COOD (500 MHz).

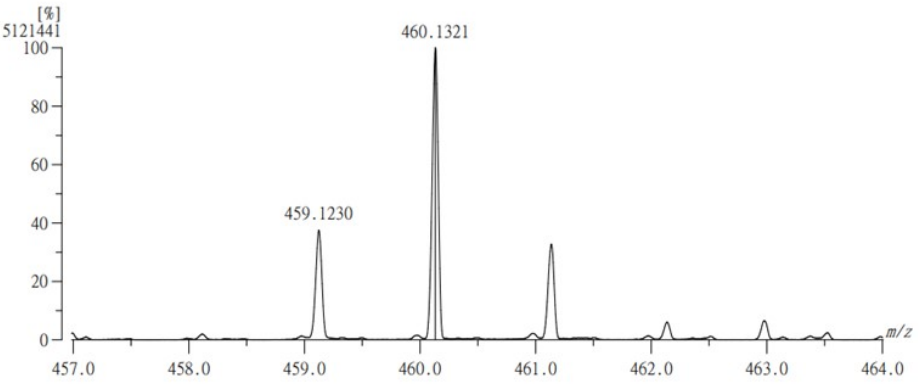

	Observed m/z	Int%	Err[ppm / mmu]	U.S.	Composition
1	460.1321	100.00	+2.2 / +1.0	26.5	C29 H14 N7
2			-0.7 / -0.3	26.0	C31 H16 N4 O
3			-3.6 / -1.7	25.5	C33 H18 N O2
4			+8.1 / +3.7	22.0	C26 H16 N6 O3
5			+5.1 / +2.4	21.5	C28 H18 N3 O4
6			-7.6 / -3.5	18.0	C20 H16 N10 O4
7			+2.2 / +1.0	21.0	C30 H20 O5
8			-10.5 / -4.8	17.5	C22 H18 N7 O5

Fig. S9 HRMS spectrum for **CNCzPyDFCN.**

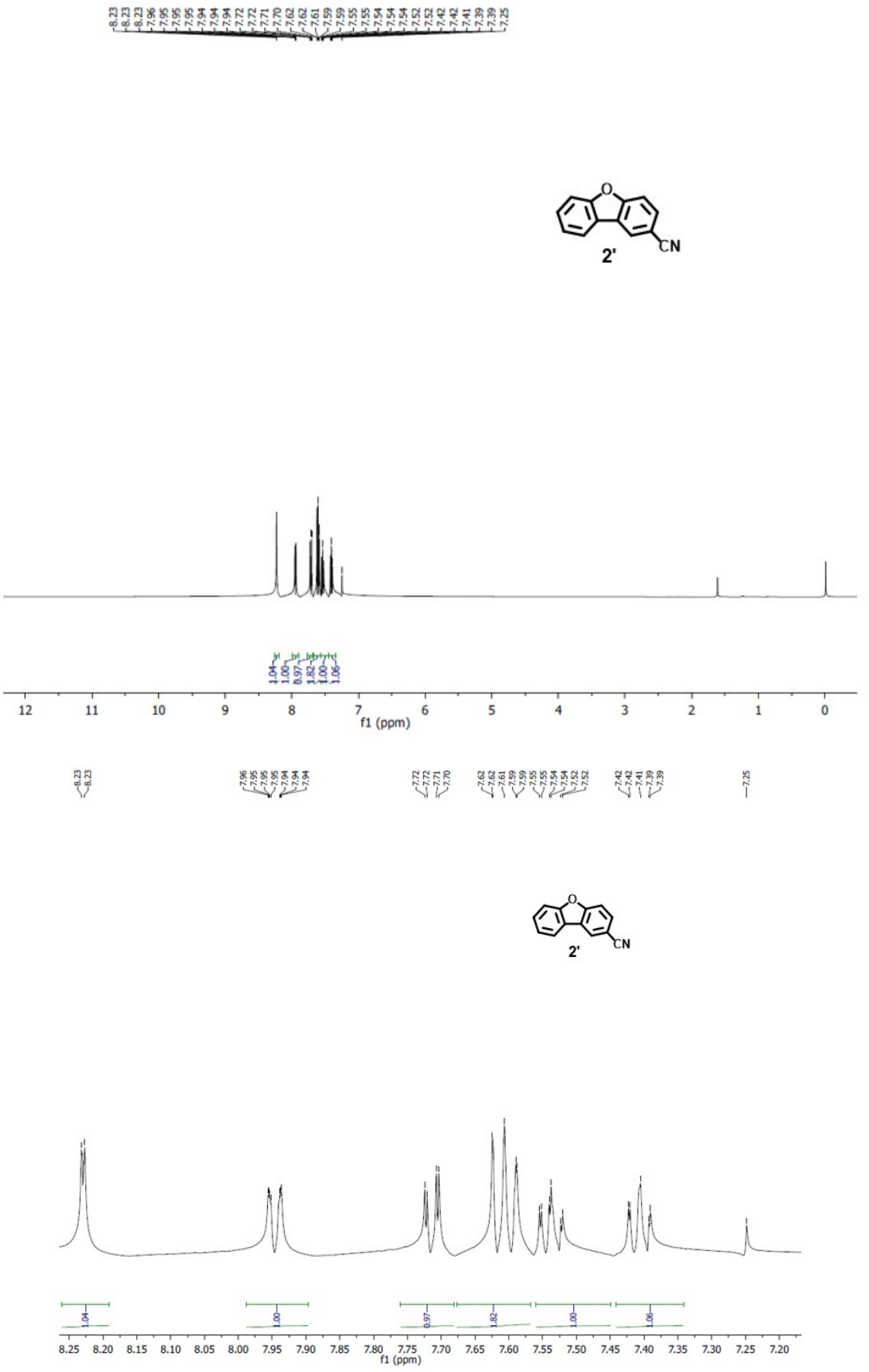

Fig. S10 ^{1}H NMR spectrum for intermediate **2'** in $CDCl_3$ (500 MHz).

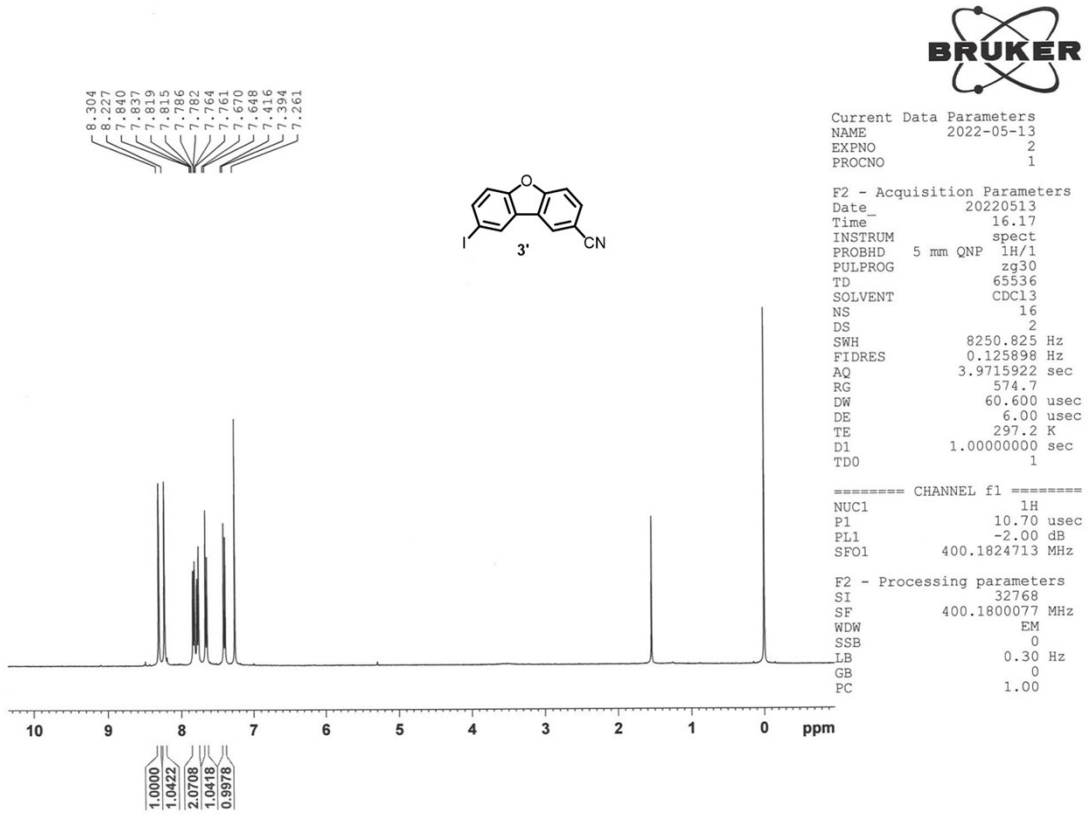

Fig. S11 ^{1}H NMR spectrum for intermediate **3'** in $CDCl_3$ (400 MHz).

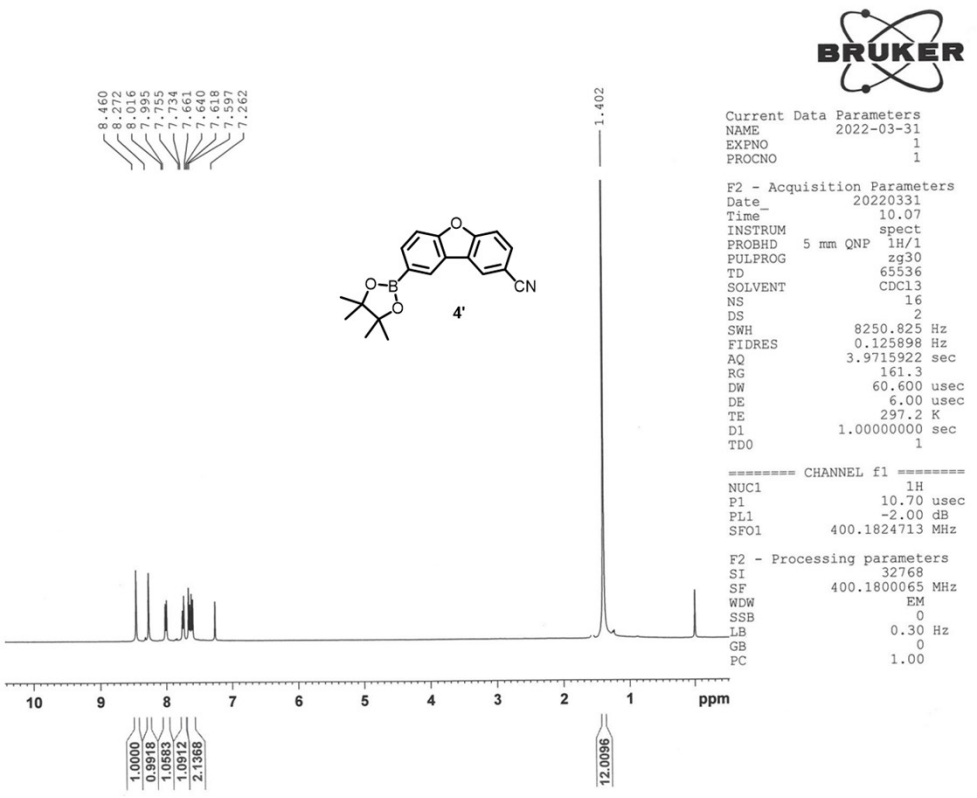

Fig. S12 ^{1}H NMR spectrum for intermediate **4'** in $CDCl_3$ (400 MHz).

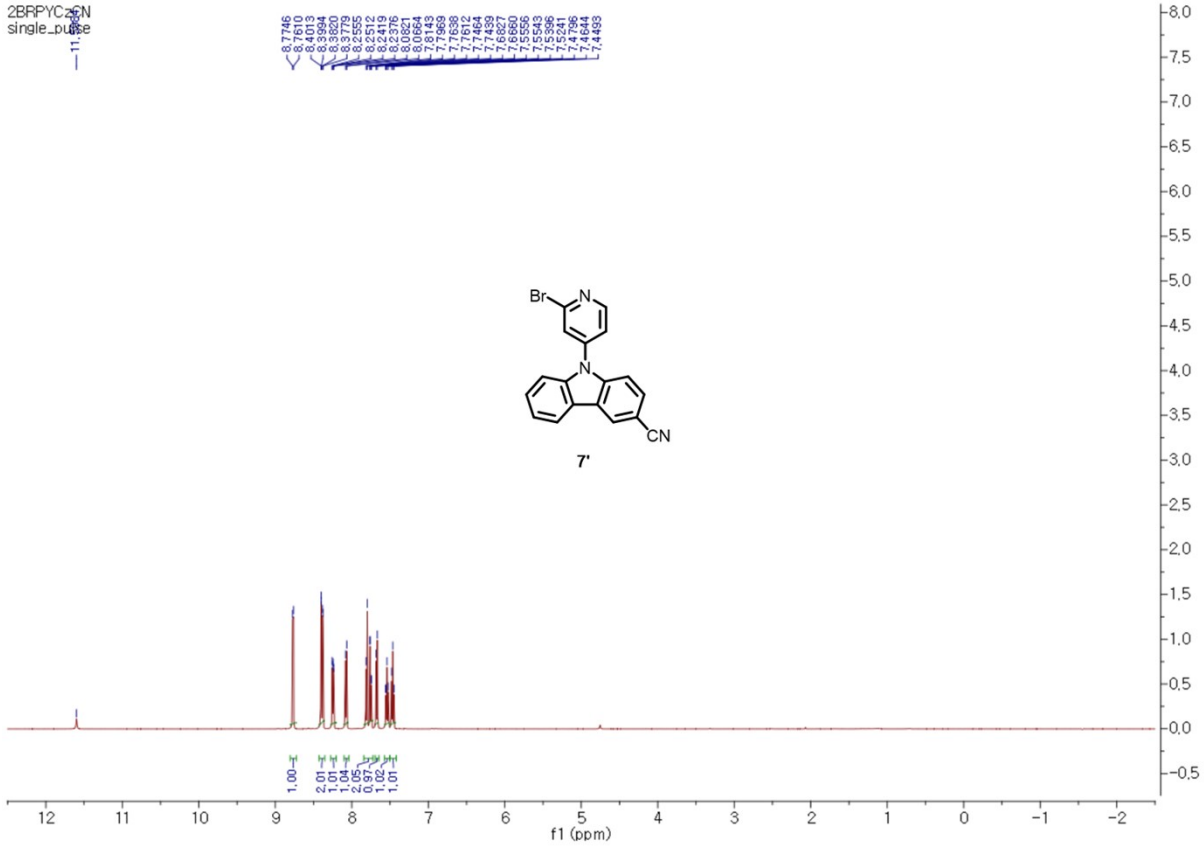

Fig. S13 ^{1}H NMR spectrum for intermediate **7'** in CF_3COOD (500 MHz).

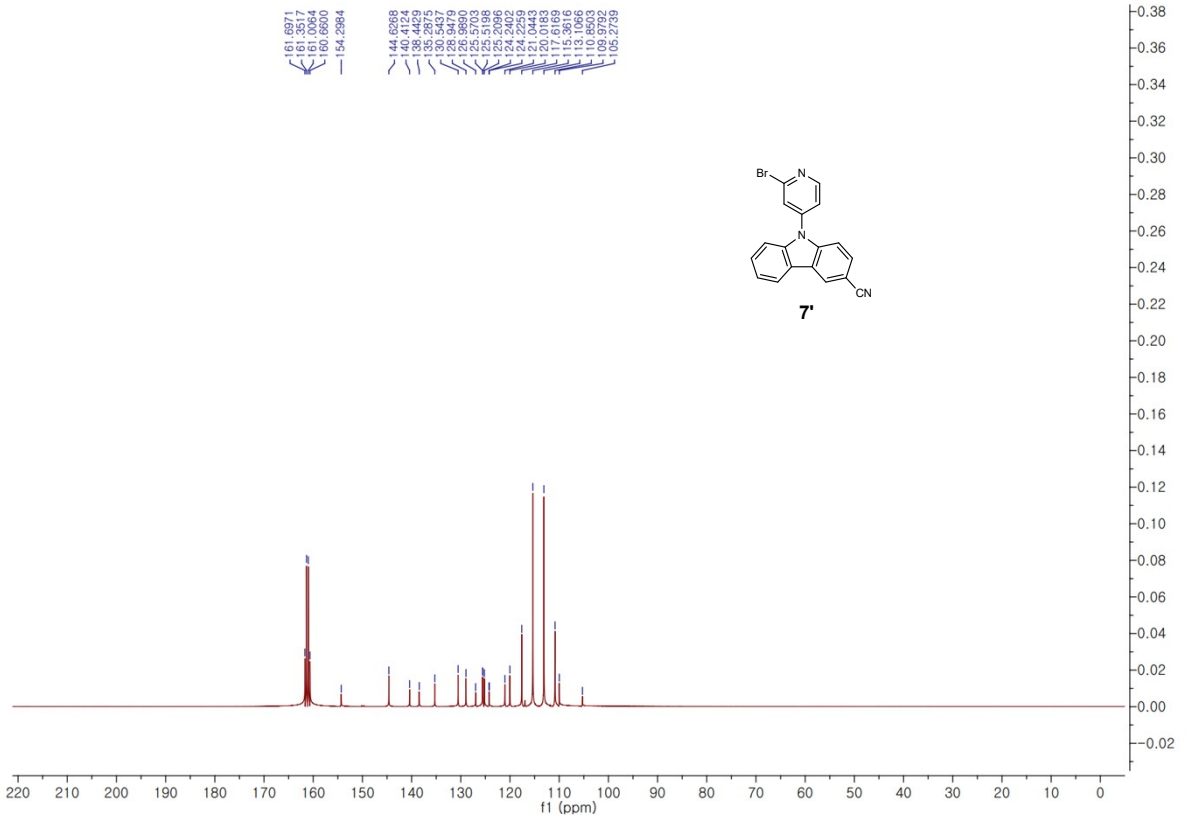

Fig. S14 ^{13}C NMR spectrum for intermediate **7'** in CF_3COOD (125 MHz).

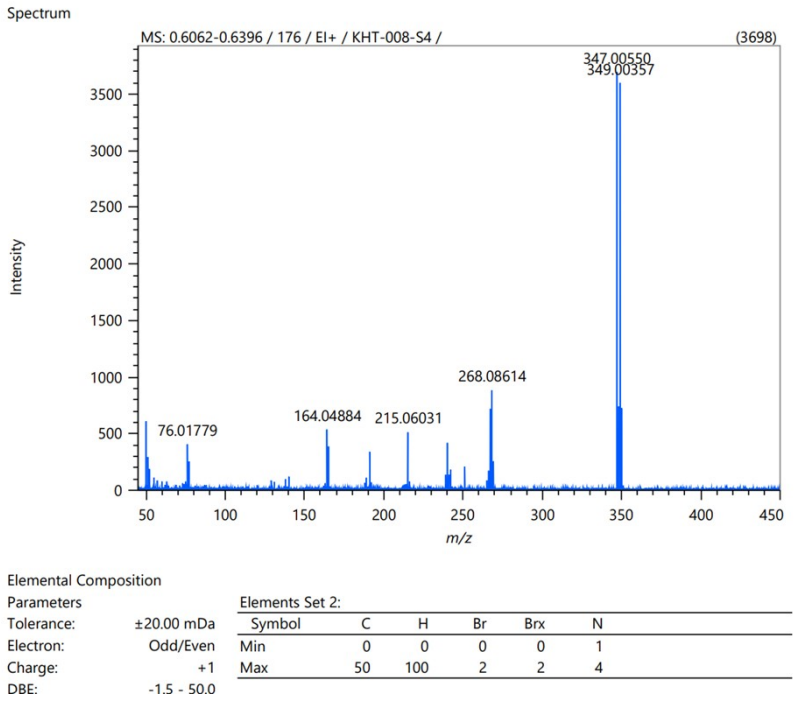

Fig. S15 HRMS spectra for spectrum for intermediate **7'**.

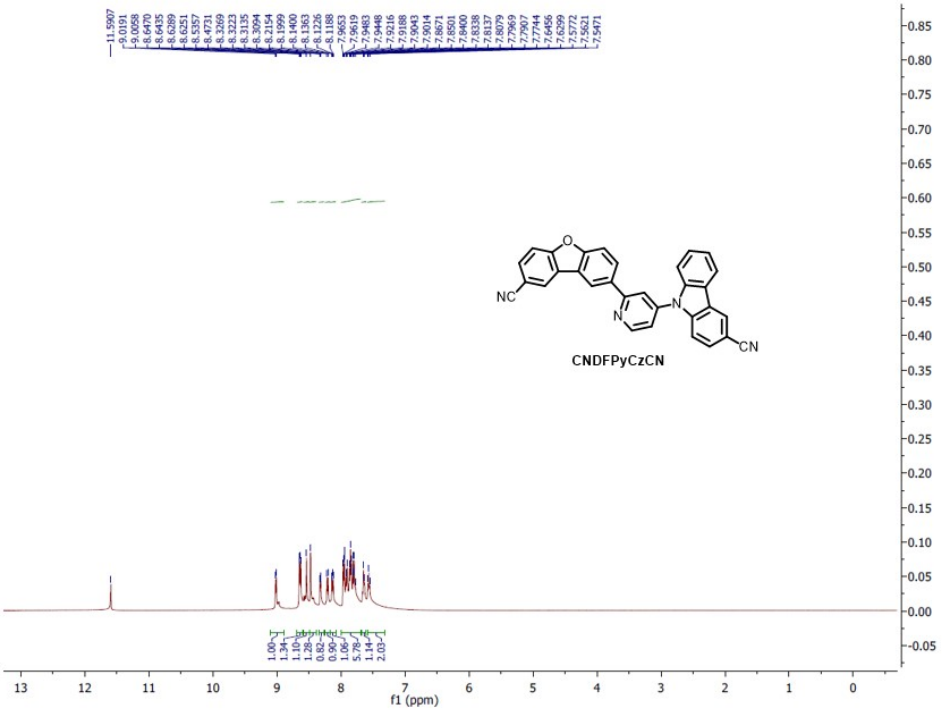

Fig. S16 ^{1}H NMR spectrum of **CNDFPyCzCN** in CF_3COOD (500 MHz).

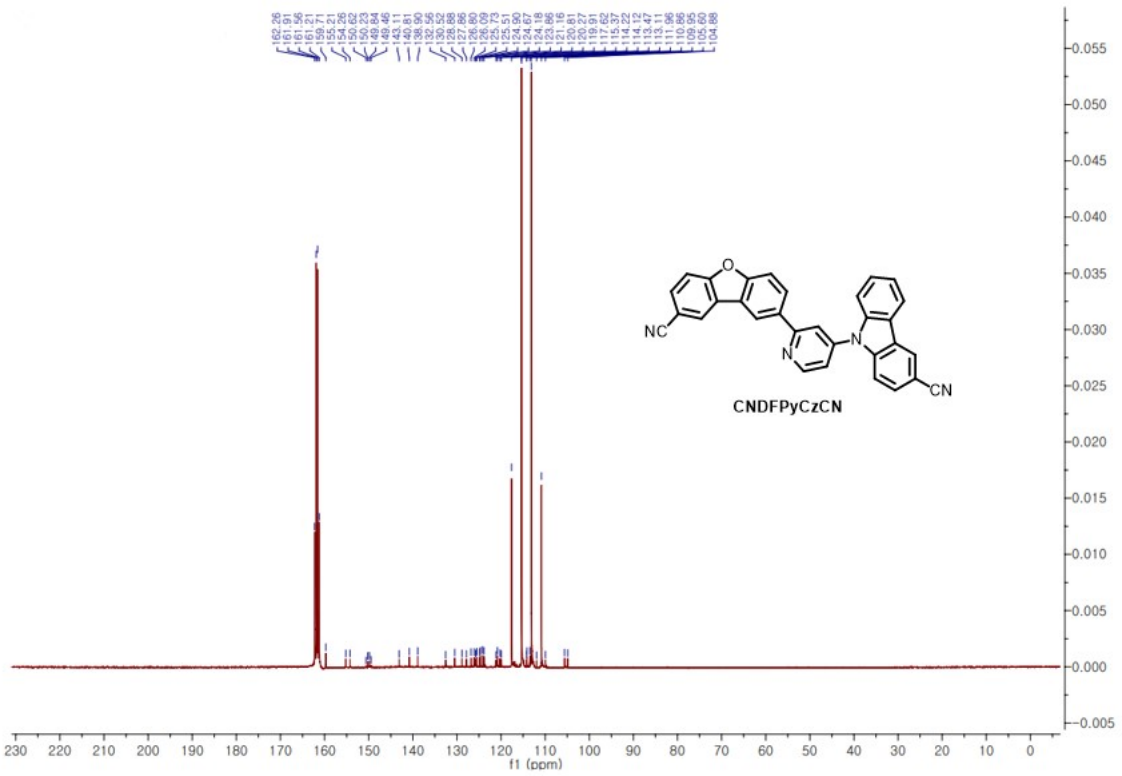

Fig. S17 ^{13}C NMR spectrum of **CNDFPyCzCN** in CF_3COOD (500 MHz).

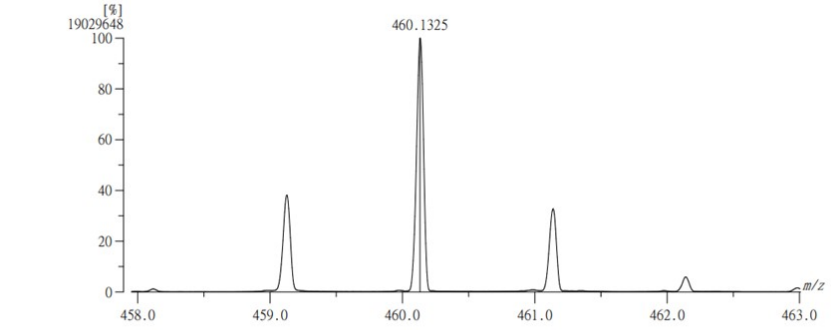

	Observed m/z	Int%	Err[ppm / mmu]	U.S.	Composition
1	460.1325	100.00	+3.1 / +1.4	26.5	C29 H14 N7
2			+0.2 / +0.1	26.0	C31 H16 N4 O
3			-2.7 / -1.3	25.5	C33 H18 N O2
4			+8.9 / +4.1	22.0	C26 H16 N6 O3

Fig. S18 HRMS spectra for **CNDFPyCzCN**.

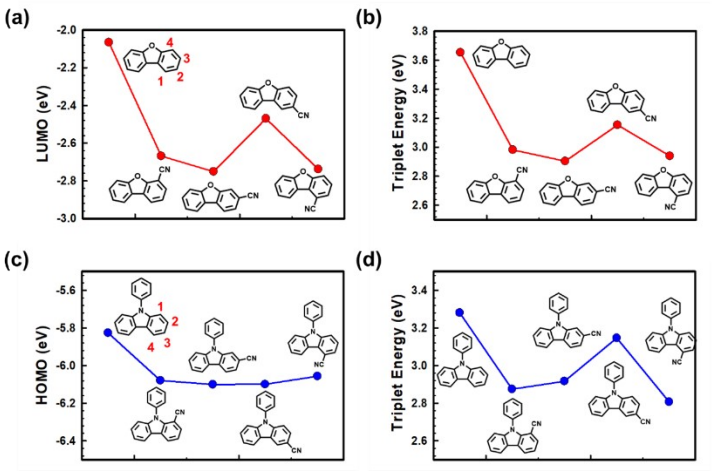

Fig. S19 Calculated (a) LUMO; (b) Triplet energy levels according to CN at various substitution positions on dibenzofuran moiety; (c) HOMO; (d) Triplet energy levels according to CN at various substitution positions on carbazole moiety through DFT simulation.

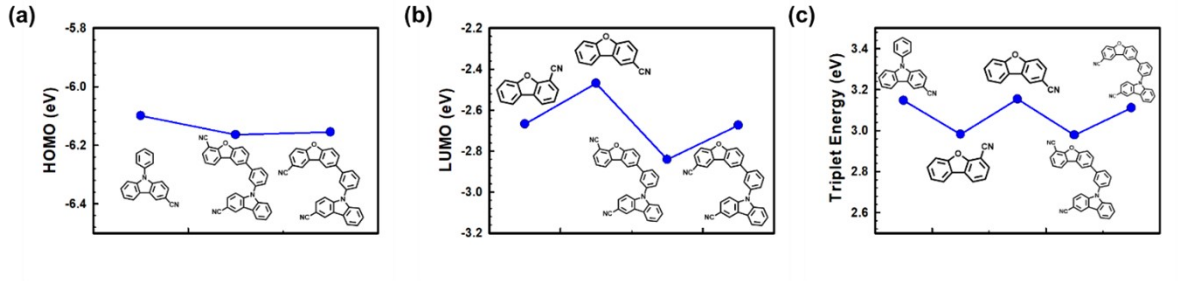

Fig. S20 Calculated (a) HOMO; (b) LUMO; (c) triplet energy level through DFT simulation.

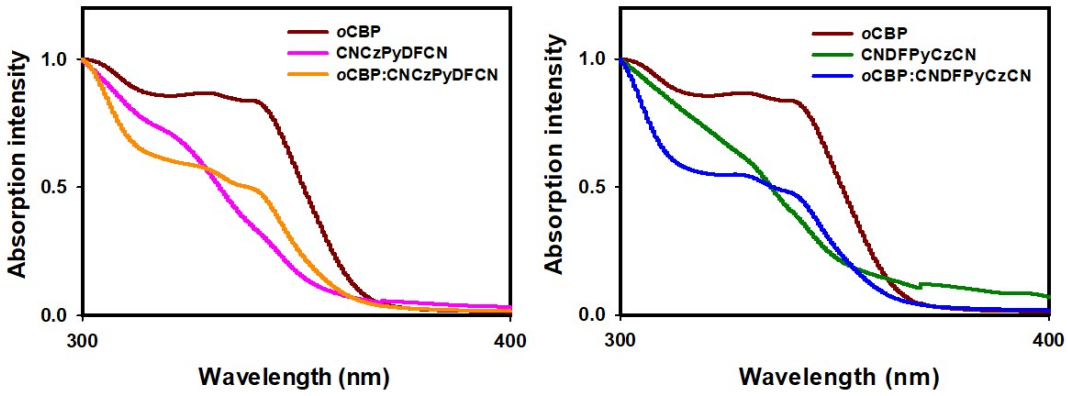

Fig. S21 Solid-state optical absorption spectra for single and exciplex host.

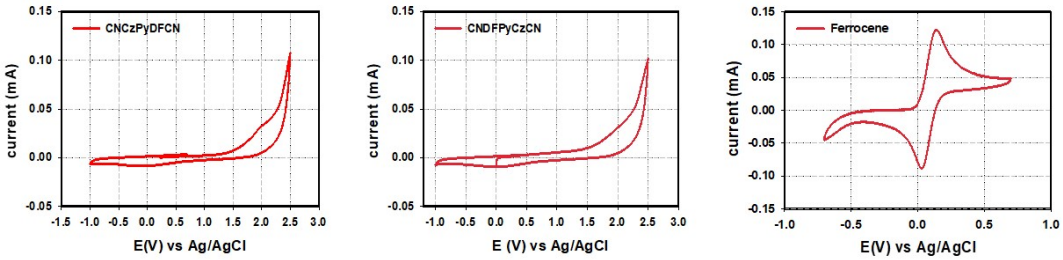

Fig. S22 Cyclic voltammetry of CNCzPyDFCN, CNDFPyCzCN, and Ferrocene coating on the ITO at the scan rate of 100 mA/s. 0.1M Tetra-*n*-butylammonium perchlorate in ACN solvent.

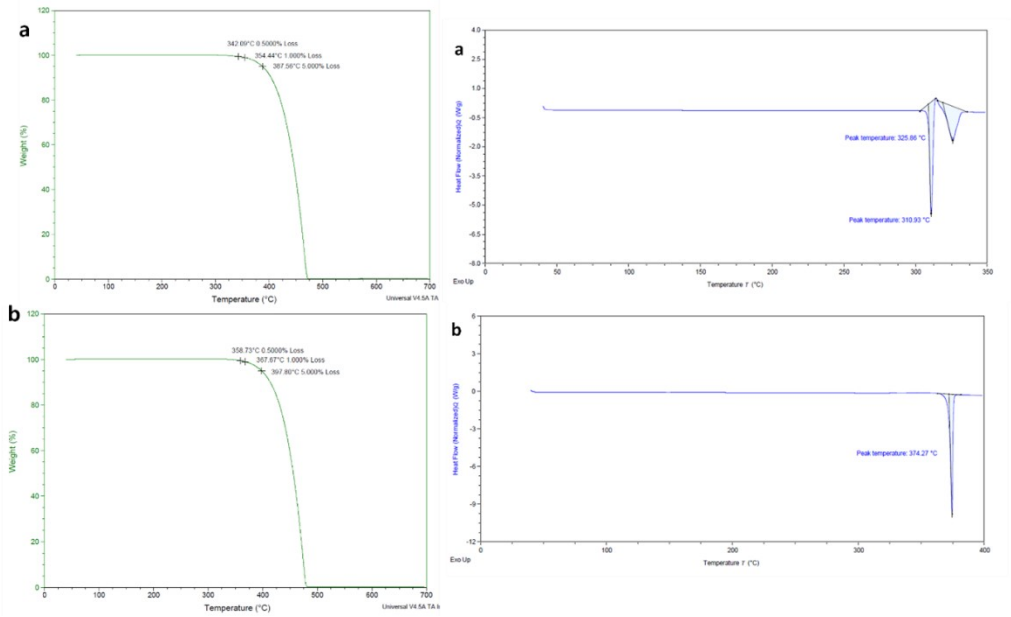

Fig. S23 TGA and DSC curves for (a) CNCzPyDFCN; (b) CNDFPyCzCN hosts.

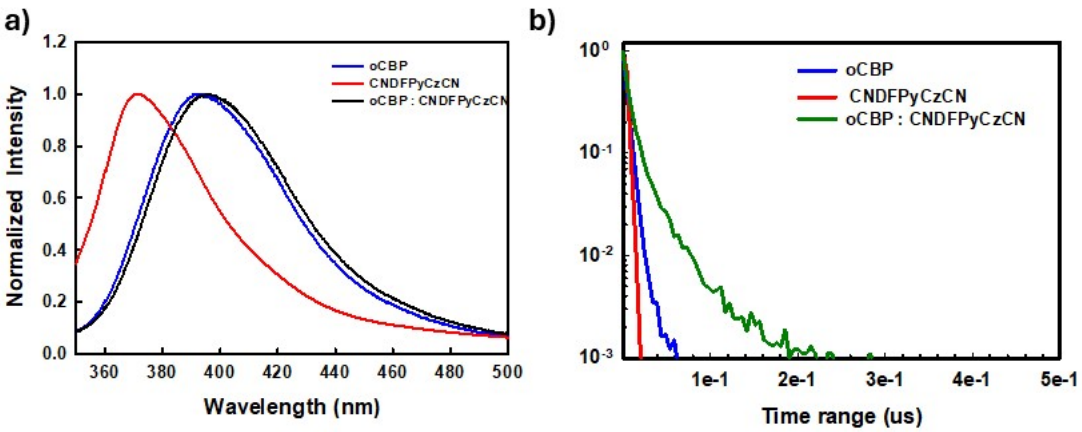

Fig. S24 (a) The solid PL spectra of *o*CBP, CNDFPyCzCN, and *o*CBP:CNDFPyCzCN mixed film with the excitation wavelength is 340 nm; (b) the transient decay curve was monitored in *o*CBP 393 nm, CNDFPyCzCN 372 nm and *o*CBP:CNDFPyCzCN 396 nm and the excitation wavelength is 340 nm.

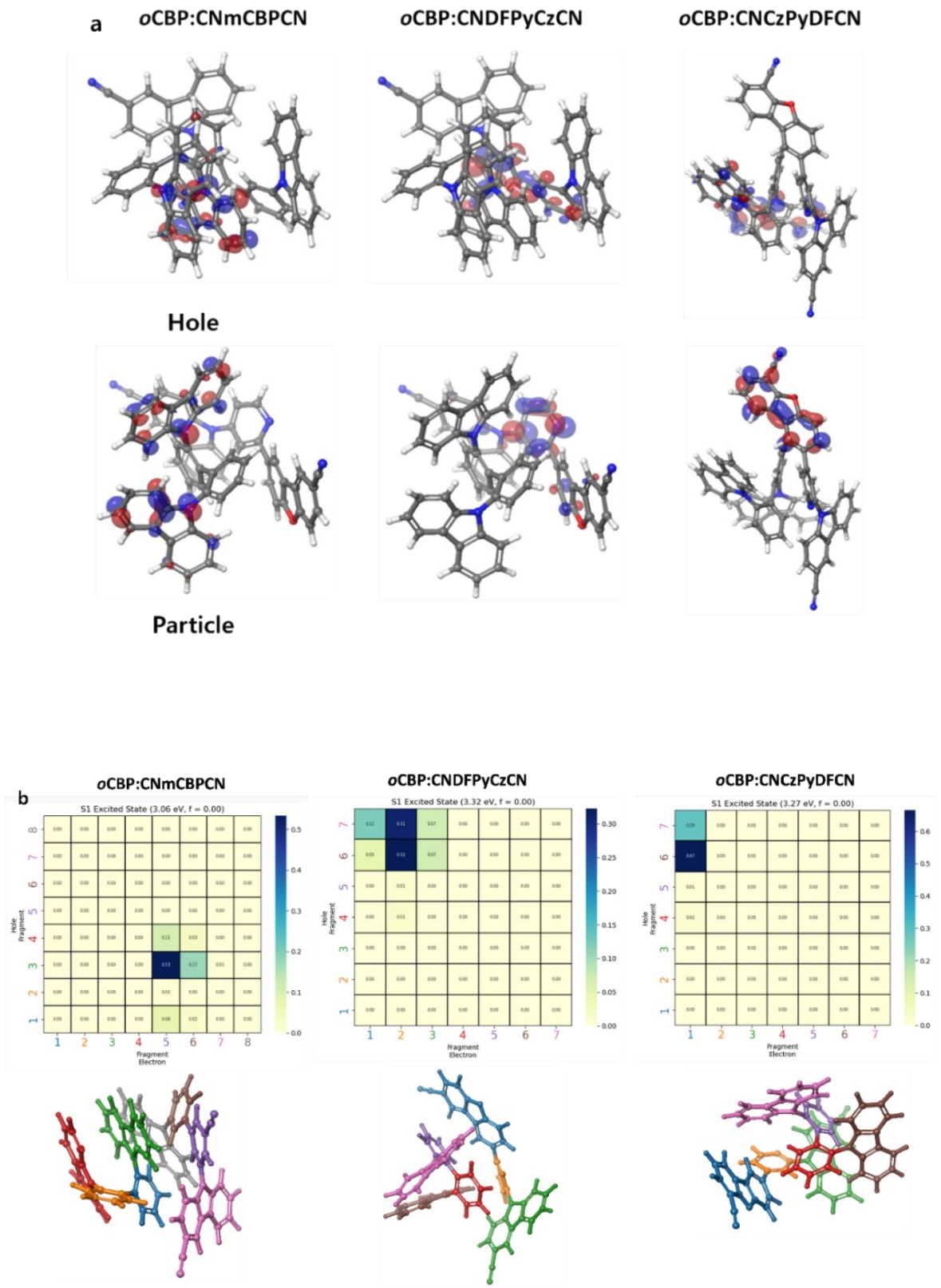

Fig. S25 (a) Natural transition orbital analysis of mixed host systems for the S1 state; (b). Excited state analysis (S1) for determining the charge transfer characteristics based on the intermolecular interaction.

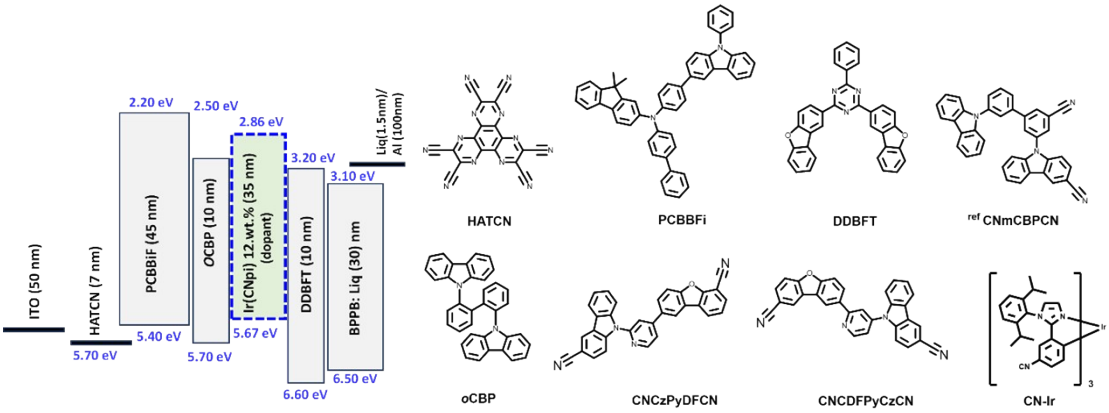

Fig. S26 Energy level diagram, device configuration, and chemical structure of OLED materials used in PhOLED devices.

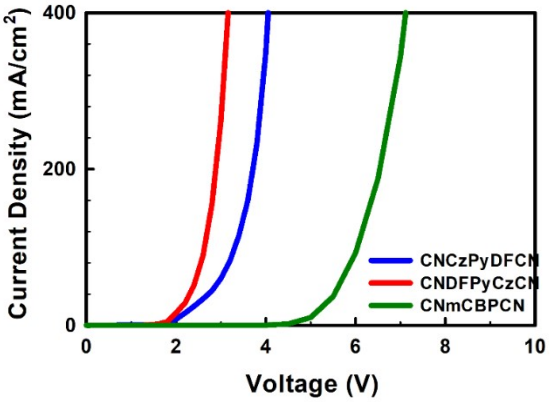

Fig. S27 Current density versus the voltage (*J–V*) curve of the electron-only device (EOD) of CNmCBPCN, CNCzPyDFCN and CNDFPyCzCN.

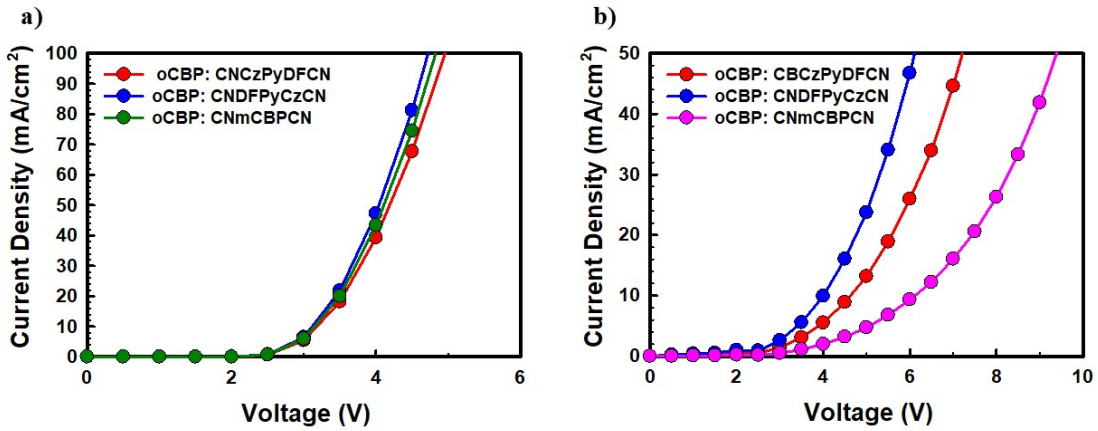

Fig. S28 Current density versus the voltage (*J–V*) curve (a) hole-only device (HOD) and (b) electron-only device (EOD) of exciplex host such as *o*CBP:CNmCBPCN, *o*CBP:CNCzPyDFCN and *o*CBP:CNDFPyCzCN.

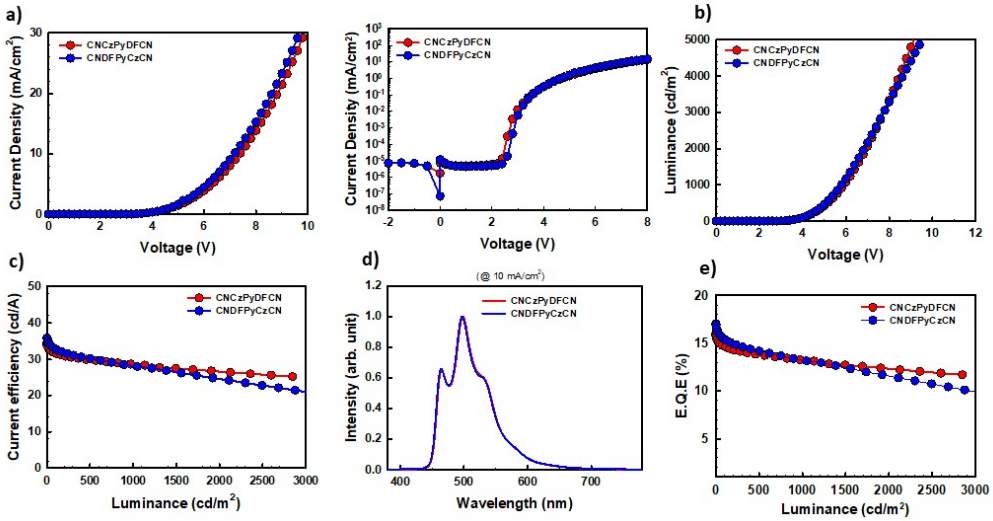

Fig. S29 (a) Current density-voltage; (b) Luminance-voltage; (c) Current efficiency–luminance; (d) EL spectra; (e) EQE Vs luminance of 12 wt% doped CN-Ir with CNCzPyDFCN, and CNDFPyCzCN at the initial luminescence of 1000 cd/m^2.

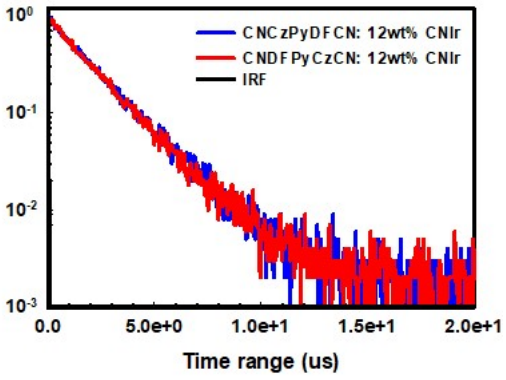

Fig. S30 The transient PL decay for doped 12. wt% of CNIr with a single host in the film state, the monitored wavelength 463 nm and excitation wavelength 340 nm.

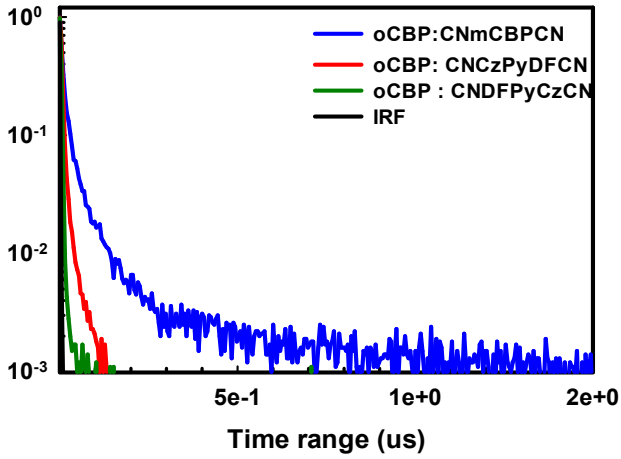

Fig. S31 TRPL data for doped 12 wt% of CNIr with exciplex co-host in the film state of *o*CBP: CNmCBPCN, (421 nm) *o*CBP: CNCzPyDFCN (423 nm) and *o*CBP: CNDFPyCzCN (396 nm) the excitation wavelength is 340 nm.

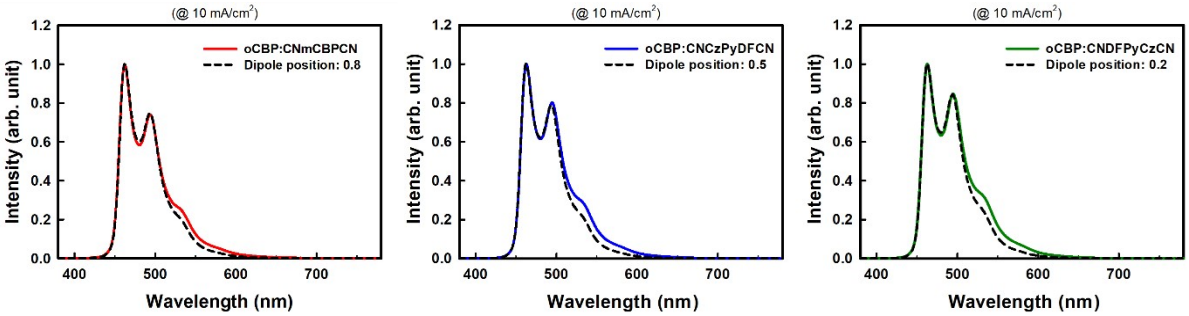

Fig. S32 The optical simulation for fitted spectra PhOLEDs.

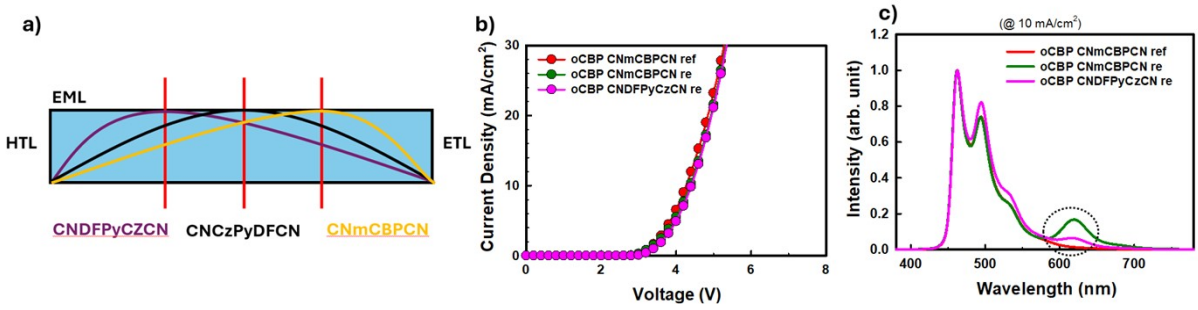

Fig. S33 (a) The dipole position of the EML hole-electron recombination zone occurred at the interface of HTL or ETL side or EML; (b) J-V characteristics; (c) EL spectra for the reference host of *o*CBP:CNmCBPCN (red for without doping and green for with doping red dopant) and *o*CBP:CNDFPyCzCN.

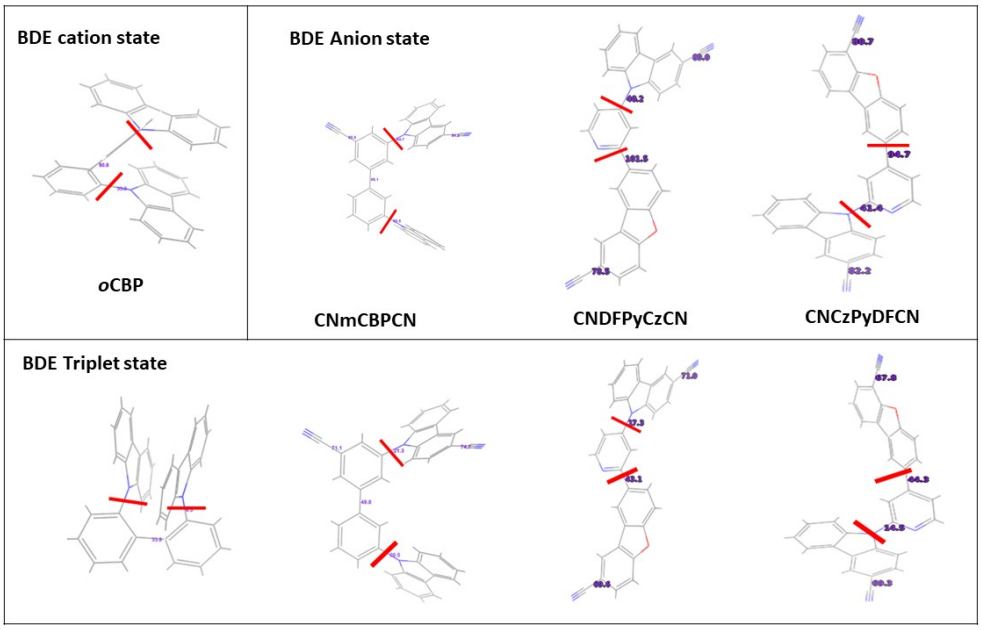

Fig. S34 The Bond dissociation energy simulation results for hole and electron transport host materials in different states such as cation, anion and triplet state.

4. Table

Table S1 Summary of photophysical parameters determined from the exciton energy transfer process for the doped CNIr with 12wt% exciplex host excitation wavelength is 340 nm.

	***o*CBP: CNmCBPCN**	***o*CBP:CNCzPyDFCN**	***o*CBP:CNDFPYCzCN**
ϕ_{PLQY}	0.165	0.204	0.219
ϕ_p	0.098	0.122	0.200
ϕ_d	0.067	0.082	0.019
ϕ_{RISC}	0.074	0.093	0.024
ϕ_{ISC}	9.02×10^{-1}	8.78×10^{-1}	8.00×10^{-1}
τ_p (ns)	3.79×10^{-8}	3.77×10^{-8}	5.20×10^{-9}
τ_d (μs)	4.50×10^{-7}	4.50×10^{-7}	7.30×10^{-8}
k_p (S^{-1})	2.64×10^7	2.65×10^7	1.92×10^8
k_d(S^{-1})	2.22×10^6	2.22×10^6	1.37×10^7
k_r(S^{-1})	2.59×10^6	3.24×10^6	3.85×10^7
k_{ISC} (S^{-1})	2.38×10^7	2.33×10^7	1.54×10^8
k_{RISC} (S^{-1})	**1.68×10^6**	**1.70×10^6**	**1.63×10^6**
k_{nr}^T(S^{-1})	2.06×10^6	2.01×10^6	1.34×10^7
k_{FET}	**1.13×10^8**	**2.29×10^8**	**1.78×10^8**
k_{DET}	3.09×10^6	3.55×10^7	1.91×10^6

ϕ_{PLQY}, photoluminescence quantum yield, τ_p, τ_d prompt, delayed lifetime, k_p, k_d, k_r and k_{nr} rate constant of prompt, delayed, radiative and non-radiative, k_{RISC} the rate of reverse intersystem crossing, k_{nr}^T is the nonradiative decay constant of triplets, k_{FET} rate of Förster energy transfer (FET) and k_{DET} rate of Dexter energy transfer (DET) were calculated from the doped film of CNIr 12. wt% with exciplex host, respectively.

Table S2 Summary of photophysical parameters determined from the exciton energy transfer process for the doped CNIr with 12wt% single host, monitored wavelength 463 nm and excitation wavelength

	CNCzPyDFCN	**CNDFPyCZCN**
ϕ_{PLQY}	0.919	0.939
τ_d (μs)	1.87×10^{-7}	1.84×10^{-7}
k_r(S^{-1})	4.91×10^5	5.10×10^5
k_{nr}^T(S^{-1})	4.33×10^4	3.31×10^4

is 340 nm.

ϕ_{PLQY}, photoluminescence quantum yield, τ_d delayed lifetime, k_r and k_{nr} rate constant of delayed, radiative and non-radiative.

Host	Dopant	EQEs (%)	CIE $_{(X, Y)}$	Lifetime (h)	Reference
*o*CBP:CNCzPyDFCN	CNIr	29.2	0.15, 0.28	LT_{50} 33.9 at 1000 cd/m^2	Current work
*o*CBP:CNDFPyCzCN		26.6	0.15, 0.29	LT_{50} 8.2 at 1000 cd/m^2	
*o*CBP:CNmCBPCN		22.9	0.15, 0.26	LT_{50} 16.4 at 1000 cd/m^2	
*o*CBP:CNmCBPCN	CNIm	18.8	0.15, 0.25	LT_{70} 366.39 at 200 cd/m^2	*J. Mater. Chem. C,* ***2018****, 6, 10308-10314*
mCBP:CzBTPCNmSi		20.0	0.16, 0.28	LT_{70} 1078 at 200 cd/m^2	*Adv. Optical Mater.* ***2022****, 10, 2101435*
*m*CBP:CNCzBTPmSi		22.6	0.16, 0.27	LT_{70} 206 at 200 cd/m^2	
*m*CBP:CNmSi-Trz		20.9	0.16, 0.29	LT_{70} 538.87 at 200 cd/m^2	
*m*CBP:CNmSi-2DBFTrz		21.4	0.16, 0.28	LT_{70} 650.50 at 200 cd/m^2	*Chem Eng J. 429,* ***2022****, 132584*
*m*CBP:CNmSi-4DBFTrz		15.9	0.16, 0.30	LT_{70} 283.03 at 200 cd/m^2	
*m*CBP:SiCN2Cz	Ir1D	23	0.20, 0.35	LT_{50} 25307 at 100 cd/m^2	*Chem Eng J. 450,* ***2022****, 137974*
CNCzPyDFCN	2.8	5.9	34.4/ 28.5	16.0/ 13.3	498/ 81 (0.19, 0.43)
CNDFPyCZCN	2.9	5.8	35.8/ 28.0	17.0/ 13.2	497/ 81 (0.19, 0.42)

Table S3 Summarized device performances from 12 wt% of CN-Ir doped ET-type host device.
[a] turn-on voltage, [b] driving voltage, [c] current efficiency, [d] external quantum efficiency, [e] maximum electroluminescence with full-width half maximum and [f] Commission Internationale de l'Eclairage coordinates.

	*o*OCBP (eV)		CNmCBPCN (eV)		CNDFPyCzCN (eV)		CNCzPyDFCN (eV)	
C-CN	BDE^+ 1.4690	BDE^T 0.2731	BDE^- 1.9317	BDE^T 0.9238	BDE^- 1.7821	BDE^T 0.5550	BDE^- 1.7431	BDE^T 0.7501
C-C					4.1063	1.9209	4.4012	1.8689

Table S4 Summary of the bond dissociation energy (BDE) in different excited states.

*m*CBP:mSiTrz		15	0.17,0.32	LT_{50} 3195 at 100 cd/m^2	
*m*CBP:mSiTrzCzCN	$Ir(cb)_3$	21.8	0.14, 0.16	LT_{50} 3750 at 100 cd/m^2	*Chem. Eur. J.* ***2021****, 27, 12642-12648*
*m*CBP:DimSi-DBFTrz		21.2	0.13, 0.16	LT_{90} 35 at 1000 cd/m^2	*J. Ind. Eng. Chem. 95* ***2021****, 260-266*
*m*CBP:mSi-DiDBFTrz		18.7	0.13, 0.16	LT_{90}18 at 1000 cd/m^2	
*m*CBP: 2Trz6CNDBF	5CzCN	15.6	0.17, 0.35	LT_{70} 61 at 500 cd/m^2	*Dyes Pigm. 187,* ***2021****, 109091*
*m*CBP: 2Trz6CNDBT		14.7	0.17, 0.36	LT_{70} 71 at 500 cd/m^2	
*m*CBP:CzBTPmSi	CNIm	23.9	0.15,0.27	LT_{50} 4364 at 100 cd/m^2	*ACS Appl. Mater. Interfaces.* ***2020****, 12, 17, 19737-19745*
*m*CBP:3CNCzBN	CN-IM	25.6	0.16,0.32	LT_{70}1,262 at 1000 cd/m^2	*Adv. Electron. Mater.* ***2020****, 6, 2000132*
*m*CBP:mSiTrz		20.3	0.16, 0.27	LT_{70} 491.03 at 1000 cd/m^2	*Adv. Opt. Mater. 7,* ***2019****, 1901374.*
DCz-OTP	DBA-DI	24.6	0.15, 0.37	LT_{90} 5.6 at 1000 cd/m^2	*J. Mater. Chem. C, 2021, 9, 7426–7435*
*o*CN-OTP		29.5	0.16, 0.38	LT_{90} 28.8 at 1000 cd/m^2	
*m*CN-OTP		21.9	0.16, 0.39	LT_{90} 9.0 at 1000 cd/m^2	
*o*CBP:mCBP-1CN	CNIr	9.1	0.15, 0.23	LT_{70} 28.66 at 200 cd/m^2	*J. Mater. Chem. C,* ***2018****, 6, 10308-10314*
DCDPA:DBFTrz	CNIr	15.3	0.14, 0.19	--	*J. Mater. Chem. C,* ***2017****, 5, 5923-5929*
t-DCDPA:DBFTrz		16.4	0.14, 0.20	--	
*m*CP:B3PYMPM	FIrpic	29.5	--	--	*Adv. Funct. Mater.* ***2015****, 25, 361-366*
*m*CP:PO-T2T		30.3	--	--	
*o*CBP:pSiTrz	$Ir(cb)_3$	18.6	0.14, 0.16	LT_{50} 1900 at 200 cd/m^2	*Adv. Optical Mater.* ***2019****, 1901374*
*o*CBP:mSiTrz		21.1	0.14, 0.16	LT_{50} 1900 at 200 cd/m^2	
*o*CBP:DBFTrz		14.4	0.14, 0.18	LT_{50} 500 at 200 cd/m^2	
CNCzCN1	CNIm	13.7	0.15, 0.26	LT_{90}130 at 200 cd/m 2	*J. Phys. Chem. C* ***2019****, 123, 14, 8531-8540*
mCB:4CzCzCN	CNIm	24.5	0.15, 0.30	--	*Chem. Commun.,* ***2019****, 55, 8178-8181*
4CzCNCzCN		25.3	0.15, 0.29	--	
24CzCzCN		22.2	0.15, 0.30	--	
24CzCNCzCN		21.4	0.15, 0.29	--	

Table S5 Summarized exciplex host utilized device performances of reported blue, fluorescent & PhOLEDs.

Table S6 Cartesian coordinates of the optimized structure of C**NCzPyDFCN** and basis set of the Lee-Yang–Parr correlation functional (B3LYP)/6-31(G)* by using the Schrodinger 2023-1 program.

Atom	**x**	**y**	**z**
N	-1.90540	4.06650	-1.83400
C	-0.96600	4.18610	-2.78570
C	0.21500	3.45110	-2.80910
C	0.49380	2.50490	-1.80510
C	-0.49970	2.37560	-0.80940

C	-1.62810	3.17800	-0.88560
C	2.90830	2.22510	-2.33160
N	-2.64220	3.07110	0.14900
C	-4.00110	2.93820	-0.08980
C	-4.67940	2.84370	1.15680
C	-3.65650	2.94420	2.19190
C	-2.41350	3.09350	1.51160
C	-4.67600	2.87090	-1.31640
C	-6.05650	2.71330	-1.28060
C	-6.74200	2.62280	-0.05370
C	-6.04970	2.68480	1.18180
C	-3.68330	2.94170	3.57370
C	-2.46690	3.09650	4.27170
C	-1.25230	3.26540	3.59360
C	-1.20150	3.27440	2.20330
C	4.11580	1.50580	-2.27290
C	4.08330	0.27050	-1.65850
C	2.91600	-0.30680	-1.09080
C	1.72050	0.43460	-1.15110
C	1.72610	1.69980	-1.77220
C	3.31000	-1.57820	-0.57200
C	4.67970	-1.68530	-0.84830
O	5.15270	-0.56180	-1.51230
C	5.47990	-2.77670	-0.50110
C	4.79220	-3.84880	0.18740
C	3.43300	-3.75910	0.46530
C	2.65310	-2.65210	0.11050
C	6.85980	-2.82790	-0.79570
N	8.00610	-2.89870	-1.02460
C	-8.16210	2.46680	-0.04600
N	-9.31890	2.34370	-0.03030
H	-1.17990	4.90810	-3.57010

H	0.91140	3.59080	-3.62760
H	-0.37480	1.65970	-0.00660
H	2.91350	3.22140	-2.76160
H	-4.14030	2.96110	-2.25140
H	-6.61950	2.66160	-2.20520
H	-6.60150	2.60540	2.11200
H	-4.61440	2.82790	4.11950
H	-2.47580	3.09220	5.35640
H	-0.33640	3.39480	4.15900
H	-0.26820	3.41860	1.67480
H	5.03900	1.90270	-2.68100
H	0.79910	0.00000	-0.77500
H	5.36190	-4.72350	0.48010
H	2.95850	-4.59100	0.98270
H	1.59350	-2.61050	0.33770

Table S7 Cartesian coordinates of the optimized structure of C**NCzPyDFCN** and the basis set of the Lee–Yang–Parr correlation functional (B3LYP)/6-31(G)* by using the Schrodinger 2023-1 program.

Atom	**x**	**y**	**z**
C	-3.02310	-0.25800	-1.12040
C	-2.42810	-1.52020	-1.19640
N	-1.19860	-1.83860	-0.81830
C	-0.38530	-0.82670	-0.28460
C	-0.89270	0.48640	-0.16330
C	-2.17900	0.75840	-0.57360

C	1.89560	-0.28000	0.66340
N	-2.68690	2.11310	-0.43910
C	-3.32070	2.62230	0.68080
C	-3.66620	3.98240	0.45230
C	-3.20600	4.29190	-0.90050
C	-2.61170	3.08830	-1.39190
C	-3.59650	1.96350	1.88150
C	-4.23640	2.69440	2.87850
C	-4.58410	4.04310	2.67140
C	-4.29870	4.70030	1.44660
C	-3.22340	5.41260	-1.70640
C	-2.65140	5.32400	-2.99710
C	-2.07260	4.13510	-3.46890
C	-2.04010	2.99480	-2.67640
C	3.17310	-0.64610	1.06340
C	3.52160	-1.98590	0.92070
C	2.63430	-2.93660	0.39580
C	1.35550	-2.56200	-0.00500
C	0.95000	-1.20700	0.12470
C	3.37160	-4.18950	0.42100
C	4.63950	-3.87720	0.96020
O	4.74630	-2.55190	1.26570
C	5.63910	-4.82430	1.14830
C	5.34990	-6.13390	0.77960
C	4.08970	-6.47570	0.23780
C	3.09310	-5.50350	0.05580
C	3.83100	-7.83590	-0.12850
N	3.62540	-8.94280	-0.42480
C	-5.23530	4.77560	3.71190
N	-5.76550	5.38360	4.55060
H	-4.03690	-0.06810	-1.44930
H	-3.01870	-2.34320	-1.60540

H	-0.28450	1.28450	0.25130
H	1.62090	0.76510	0.77040
H	-3.31510	0.92670	2.01960
H	-4.47070	2.22880	3.82900
H	-4.57680	5.74090	1.31910
H	-3.65990	6.34780	-1.36970
H	-2.66020	6.20080	-3.63670
H	-1.64350	4.10890	-4.46470
H	-1.59890	2.06410	-3.01050
H	3.87140	0.07900	1.46920
H	0.65020	-3.27530	-0.41230
H	6.60170	-4.54910	1.56590
H	6.09580	-6.91180	0.90640
H	2.12990	-5.78050	-0.36050

5. References

1. S. L. Gong, X. He, Y. H. Chen, Z. Q. Ziang, C. Zhong, D. G. Ma, J. G. Qin, C. L. Yang, *J. Mater. Chem*. 2012, **22**, 2894.
2. Y. J. Kang, S. H. Han, J. Y. Lee, *J. Ind. Eng. Chem*. 2018, **62**, 258.
3. S. Jang, K. H. Lee, S. Hong, J. Y. Lee, Y. Lee. *Dyes Pigm*. 2021, **187**, 109091.
4. S. Ihn, D. Jeong, E. S. Kwon, S. Kim, Y. S. Chung, M. Sim, J. Chwae, Y. Koishikawa, S. O. Jeon, J. S. Kim, J. Kim, S. Nam, I. Kim, S. Park, D. S. Kim, H. Choi, S. Kim, *Adv. Sci*. 2022, **9**, 2102141.